THE SPECTRAL RESPONSE OF SOME INORGANIC PHOSPHORS TO FAST IONS

A Thesis Presented in Partial Fulfillment of the Requirements

for the

Degree of Master of Science

at

Lakehead University

Ee-hua Goh

Lakehead University

1972

Canadian Theses on Microfilm No. 16721

ABSTRACT

Photoluminescent spectra of thin powdered $Zn_2SiO_4:Mn$ (P-1), $CaWO_4$ (P-5), $ZnS:Ag$ (P-11 and P-22), $ZnCdS:Ag$ (P-20 and P-22) and $ZnS:Ag:Cu$ (P-2 and P-31) samples excited by ultra-violet radiation of wavelengths 2537 A, 3130 A and 3650 A were compared with the ionoluminescent spectra excited by H^+, He^+, N^+, Ne^+ and Ar^+ beams in the energy range of 10 - 100 KeV. Except for $ZnS:Ag:Cu$ the ionoluminescent spectra were similar to the photoluminescent spectra in their spectral energy distribution. The energies of the emission peaks of all the luminophors studied were not sensitive to the energy or mass of the incident projectile. The relative intensity of the green and blue peaks of $ZnS:Ag:Cu$ was found to depend strongly on ion energy, ion mass and the dosage of the ion.

ACKNOWLEDGEMENTS

I would like to express my appreciation to Dr. Lynden Hastings for his assistance in my work and in the preparation of this thesis.

I would also like to thank Dr. V. V. Paranjape and Professor B. J. Spenceley for their kind help in various respects.

I am also grateful to Mr. G. Anderson for his remarkable technical skill in building the second target chamber.

LIST OF FIGURES

LIST OF TABLES

TABLE OF CONTENTS

[PAGE]

I

INTRODUCTION

Although the phenomenon of luminescence was observed as long ago as 1603,[1] it was not well understood until the investigative techniques and concepts of solid state physics were applied in the second quarter of this century. The study of fast ion induced luminescence or ionoluminescence is still in its early stages in comparison to luminescence induced by electrons or ultra-violet light. This has resulted in part from the fact that the mechanisms by which a fast, heavy ion interacts with a solid are much more complicated than those by which photons or electrons interact.

The present work was undertaken to investigate the spectra produced by various luminophors under positive ion bombardment. The ionoluminescent spectra of Zn_2SiO_4:Mn (P-1), $CaWO_4$ (P-5), ZnS:Ag (P-11 and P-22), ZnCdS:Ag (P-20 and P-22) and ZnS:Ag:Cu (P-2 and P-31) were compared to their ultra-violet spectra. For all of the luminophors studied with the exception of ZnS:Ag:Cu luminophor, the spectral energy distribution of the emission under ion excitation was found to be similar to that produced by ultra-violet excitation. The spectral energy distribution is independent of ion energy and mass within experimental limits.

ZnS:Ag:Cu is a luminophor which exhibits a blue peak and a green peak in its ionoluminescent spectrum. The relative intensity of these two peaks was found to depend strongly on ion energy, mass

and dosage, and for this reason, this luminophor was examined more closely than the others. The procedure of normalizing the spectra in terms of the total light output made it impossible to detect such effects in a simple phosphor.

II

REVIEW OF RECENT WORK

Most of the work done with ion bombardment has been concerned with the energy and mass dependence of the light output and with the modification of the luminescent properties of the luminophors produced by the bombardment. Hanle and Rau[2] studied the luminescence response of *ZnS:Ag* as a function of ion energy in the range 15-35 KeV. Richards and Hay[3] observed the light output as a function of energy for K^+ and Rb^+ with energies up to 35 KeV. Eve and Duckworth[4] studied the luminescence response of *ZnS:Ag* and Zn_2SiO_4 bombarded by H^+, Li^+, Na^+, K^+, A^+ and Rb^+ ions (E < 25 KeV) as a function of ion energy. Van Wijngaarden, Bradley and Finney[5] studied the luminescence response of *MgO* and Zn_2SiO_4*:Mn* bombarded by the same series of ions as a function of ion energy in the range of 2 KeV < E < 90 KeV. By comparing the luminescence response to ion excitation in the damaged and undamaged portion of the *ZnS:Ag* luminophor surface, the total average energy loss of ^1H, ^4He, ^{14}N, ^{40}Ar and ^{84}Kr, in passing through the films, was determined by Hastings, Ryall and van Wijngaarden.[6] Luminescence of *SiC* single crystal was studied with H^+, H_2^+, D^+, D_2^+ and D_3^+ bombardment by Makarov and Petrov.[7] In the present study, the ionoluminescence spectra of the various luminophors were observed in the energy range of 7.5 KeV to 162 KeV at room temperature.

III

THEORY

Theory of Luminescence

The configuration coordinate model proposed by von Hippel[8] still provides a good theoretical basis for the explanation of the mechanism of the various luminescent processes.

The diagram (shown on page 5) is similar to that given by Seitz[9] to account for the luminescence of *KCl:Tl*. The ordinate represents the total energy of the system in which *Tl* is the luminescence center. The configuration coordinate represents changes in the average internuclear spacings and possible changes in the geometric arrangement of the atoms or ions in the system of the center. This is, by first approximation, characterized by the distance of the Tl^+ ion from the neighbouring ions as the overlap of the wave function is small.

The center is in the ground state A initially. If the center is excited, say, by absorbing a photon of sufficient energy, an electronic transition of the impurity ion occurs. The center is then raised to an excited state at B. According to the Frank-Condon principle, the electronic transition occurs in a time short compared with that necessary for an ion to move appreciably; hence, the transition is a vertical one. After reaching the excited state, the center tends to move in such a way as to attain a new equilibrium at C, by emitting a phonon. The center will then return to its ground state at D by emitting a photon if the transition is not forbidden. This step produces the luminescent emission. The center will ultimately come back to point A

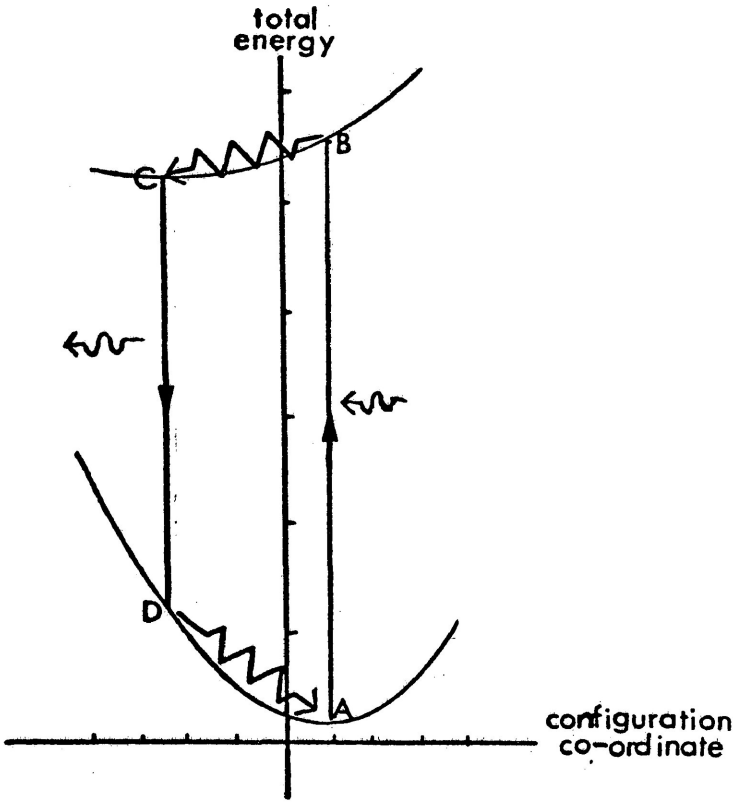

Fig. 1. The configuration coordinate model.

by phonon emission as the system returns to equilibrium.

ZnS crystallizes in the cubic zinc blende structure at low temperature and the hexagonal wurtzite structure at about 1020°C. The nature of the chemical bond is a mixture of about 50% ionic and 50% covalent bond.[9] It is known that the broad band emission of *ZnS* luminophor is due to the activators and co-activators incorporated in the compounds.[10] Several other models have been suggested for luminophors of this type.

A well-known model of the luminescence mechanism in these compounds was proposed by Schön[11] and Klasens.[12] Luminescence was attributed to an electronic transition from the conduction band to a localized level above the valence band. Fig. 2 illustrates the Schön-Klasens model. Emission occurs when a conduction electron is captured by an empty center.

Lambe and Klick[13,14] proposed another model which asserted that luminescence emissions resulted from the capture and subsequent recombination of a free hole from the valence band to a localized level below the conduction band. Fig. 3 is an illustration of this model.

Prener and Williams[15,16] found that copper at random zinc sites in *ZnS*, prepared by radioactive decay of ^{65}Zn produced by neutron irradiation, did not contribute to the luminescent emission. Luminescent transitions were attributed to associated activator-co-activator pairs consisting of second and third nearest neighbours. Fig. 4 illustrates the Prener-Williams model. An electron from the donor level recombines with a hole in the associated acceptor level and emission occurs. The donor-acceptor pair emissions were observed by

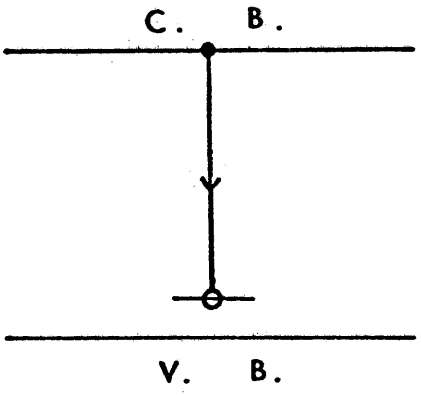

Fig. 2. The Schön-Klasen model.

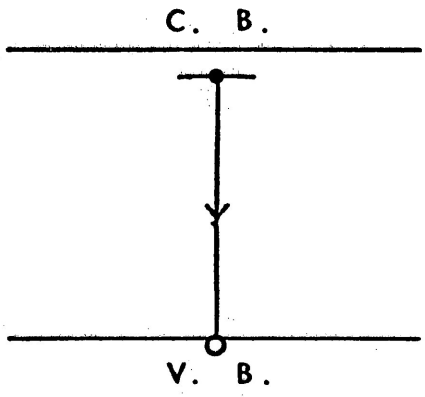

Fig. 3. The Lambe-Klick model.

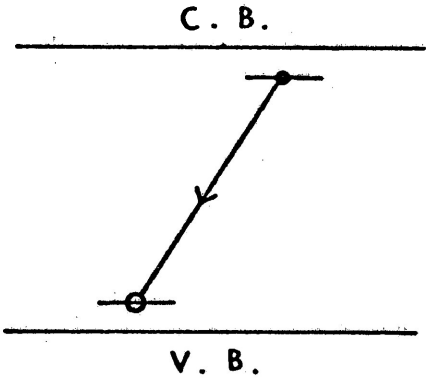

Fig. 4. The Prener-Williams model.

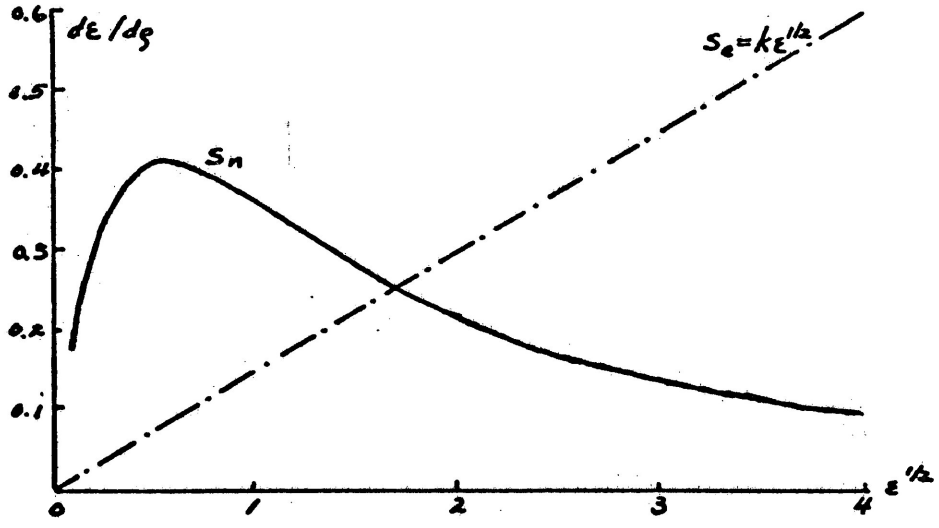

Fig. 5. The nuclear and electronic energy loss (from Lindhard *et al.*[25]).

several workers (see, for instance, Hopfield,[17] Thomas *et al.*,[18,19] Ryan and Miller[20]). Era, Shionoya and Washizawa[21] studied the spectral shift during luminescent decay and that with excitation intensity for the broad band emission in *ZnS* luminophors. The green band of *Cu*-activated *ZnS*, the blue band of *Ag*-activated *ZnS* and that of the self-activated *ZnS* were concluded to be due to the donor-acceptor pair emission mechanism.

Energy Loss and Ionoluminescence

When a solid is traversed by an energetic particle, energy is lost by the particle in both electronic and nuclear collisions. Electronic collisions produce electronic excitation or the ejection of the electron from the lattice atoms. If the solid is a luminophor, luminescence emission occurs if the excited electron or the free electron is captured by a hole through a radiative recombination process. Nuclear collisions cause the target atoms to recoil. If the energy transfer is small, the target atom will relax to its initial position by phonon emission. If the energy transfer is sufficiently large (above $\simeq$ 25 eV), the defects produced by the nuclear collisions may form non-radiative recombination centers and the luminescent efficiency of the material will decrease.[22]

For low energy (KeV) ion bombardment, the energy loss per unit distance traversed, or the stopping power, of a stopping material is usually considered as the sum of the electronic and nuclear components, i.e.

$$-dE/dX = (-dE/dX)_e + (-dE/dX)_n \quad . \qquad \text{(III.1)}$$

The stopping cross-section, S, is related to the stopping power by

$$-dE/dX = NS \qquad \text{(III.2)}$$

where N is the number of atoms per unit volume of the stopping material. Hence

$$S = S_e + S_n \qquad \text{(III.3)}$$

with the subscripts e and n referring to the electronic and nuclear components, respectively.

Both S_e and S_n have been studied extensively by Lindhard and his co-workers.[23-26] According to Lindhard *et al.*[26] nuclear collisions dominate when the ion penetrates a medium at a velocity very much smaller than the orbital velocity of an electron which could be carried by the ion, i.e.

$$v \ll v_1 = Z_1^{2/3} v_0 \qquad \text{(III.4)}$$

where Z_1 is the atomic number of the penetrating ion and v_0 is the velocity of an electron in the first Bohr orbit. At increasing velocities, the electronic collisions become more and more predominant, especially for $v \gtrsim v_1$. The electronic and nuclear stopping powers are of the same order of magnitude when $v \sim 0.1\ v_1$.[25]

Fig. 5, a reproduction of a curve presented by Lindhard *et al.*,[24] is a plot of the differential energy loss, $d\varepsilon/d\rho$, *versus* $\varepsilon^{1/2}$ where the variables

$$\rho = RNM_2 \cdot 4\pi a^2 M_1 / (M_1 + M_2)^2 \qquad \text{(III.5)}$$

and

$$\varepsilon = aM_2 E / Z_1 Z_2 e^2 (M_1 + M_2) \qquad \text{(III.6)}$$

were introduced as dimensionless measures of range R and energy E, respectively. M, A, Z and e are the mass, mass number, atomic number and electronic charge, respectively. The subscripts, 1 and 2, refer

to the incident and target atoms, respectively. The screening parameter a is given by

$$a = 0.8853\, a_0 (Z_1^{2/3} + Z_2^{2/3})^{-1/2} \qquad \text{(III.7)}$$

where a_0 is the radius of the first Bohr orbit for a hydrogen atom. The curves were derived by assuming a Thomas-Fermi potential between the colliding atoms. s_n and s_e are the differential energy losses for the nuclear and electronic collisions, respectively. S_e was found to be proportional to the velocity and is given approximately by

$$S_e = \zeta_e\, 8\pi e^2 a_0 \frac{Z_1 Z_2}{Z} \left(\frac{V}{V_0}\right)$$

$$= \zeta_e\, 8\pi e^2 a_0 \frac{Z_1 Z_2}{Z} \sqrt{\frac{E}{E_0}} \qquad \text{(III.8)}$$

where

$$Z^{2/3} = Z_1^{2/3} + Z_2^{2/3}, \qquad \text{(III.9)}$$

E is the initial energy when a projectile enters the stopping medium, E_0 is the kinetic energy of the projectile when its speed equals v_0, and ζ_e is a constant having a value between 1 and 2.[22]

Van Wijngaarden *et al.*[5] proposed that the light produced by a luminophor should be given by

$$L(E) = C \left| \int_0^E \frac{S_e}{S_e + S_n}\, dE \right| \qquad \text{(III.10)}$$

where the constant C depends upon factors such as the efficiency of the luminophor and perhaps the ion velocity. This formula predicted the results for some luminophors, but agreement for ZnS types was not good. Recently Hastings and his co-worker[27] have had considerable success in

theoretically describing the light output of ZnS type luminophors using this equation and considering the effect of non-radiative surface recombination in a manner similar to Makarov and Petrov.[7]

IV

APPARATUS AND PROCEDURE

Samples

Powdered $Zn_2SiO_4:Mn$ (P-1), $CaWO_4$ (P-5), $ZnS:Ag$ (P-11 and P-22) and $ZnS:Ag:Cu$ (P-2 and P-31) made by General Electric and supplied by Alfa Inorganics were suspended in methanol. A quantity of one of these suspensions was then poured into a large diameter burette in which a clean quartz plate was hung. The suspension was allowed to settle for a few seconds and then drained slowly so that a thin uniform layer of the sample was deposited on the quartz surface. The methanol was then allowed to evaporate thoroughly from the sample.

Photoluminescence

A vacuum ultra-violet scanning spectrometer (Jarrell-Ash, type 78-751, grating specification: 1.0 meter radius of curvature, 590 groove/mm, 80 × 40 mm ruled area, 1500 Å blaze) was used to resolve the luminescent spectra. Light from an ultra-violet source (*Hg-Zn-Cd*, Philips, type 93146E) was passed through mercury line interference filters (Oriel Optics, model G-521-2537, G-521-3130 or G-521-3650, 1 in. diameter which passed the 2537 Å, 3130 Å and 3650 Å lines, respectively) and then allowed to impinge upon luminophor samples mounted in front of the entrance slit of the spectrometer. One of a series of ultra-violet neutral density filters (Oriel Optics, model G-66-22, G-66-24, G-66-26, G-66-27 and G-66-28, all 1 in. diameter)

was inserted between the mercury line interference filter and the light source to reduce the excitation intensity. The emission spectra were detected with an EMI type 9635A photomultiplier. The output of the photomultiplier was measured by a Keithley 410A Picoammeter and recorded by a Mosley model 7100B strip chart recorder. Both the entrance and exit slits of the spectrometer were kept as narrow as possible consistent with a reasonable spectral intensity. The settings were both 30 μm.

Ionoluminescence

The ion-accelerator and magnetic analyzer used for observing the ionoluminescence spectra are outlined in Fig. 6. The ions were produced in an electron bombardment source and accelerated between slits S_1 and S_2 by a Universal Voltronics model BAL-130-1.5 LU power supply, H.V. After acceleration, the beam, collimated by slit S_3, entered a magnetic field, B, for separation into its mass components. The desired ion beam was bent through an angle of 30° along a circular path of 35 in. radius. The beam was then further collimated by S_4. The luminophor sample, attached to the bottom of a Faraday cup, F, was then bombarded by the focused ion beam. The Faraday cup and sample could be moved by means of a bellows to allow measurement of the ion current. Slit S_5 was maintained at a negative potential of 22½V to prevent the escape of secondary electrons from the Faraday cup. The ion beam current was measured by a Keithley type 416 High Speed Picoammeter connected to the cup.

In the preliminary experiments, the entrance slit of the ultra-

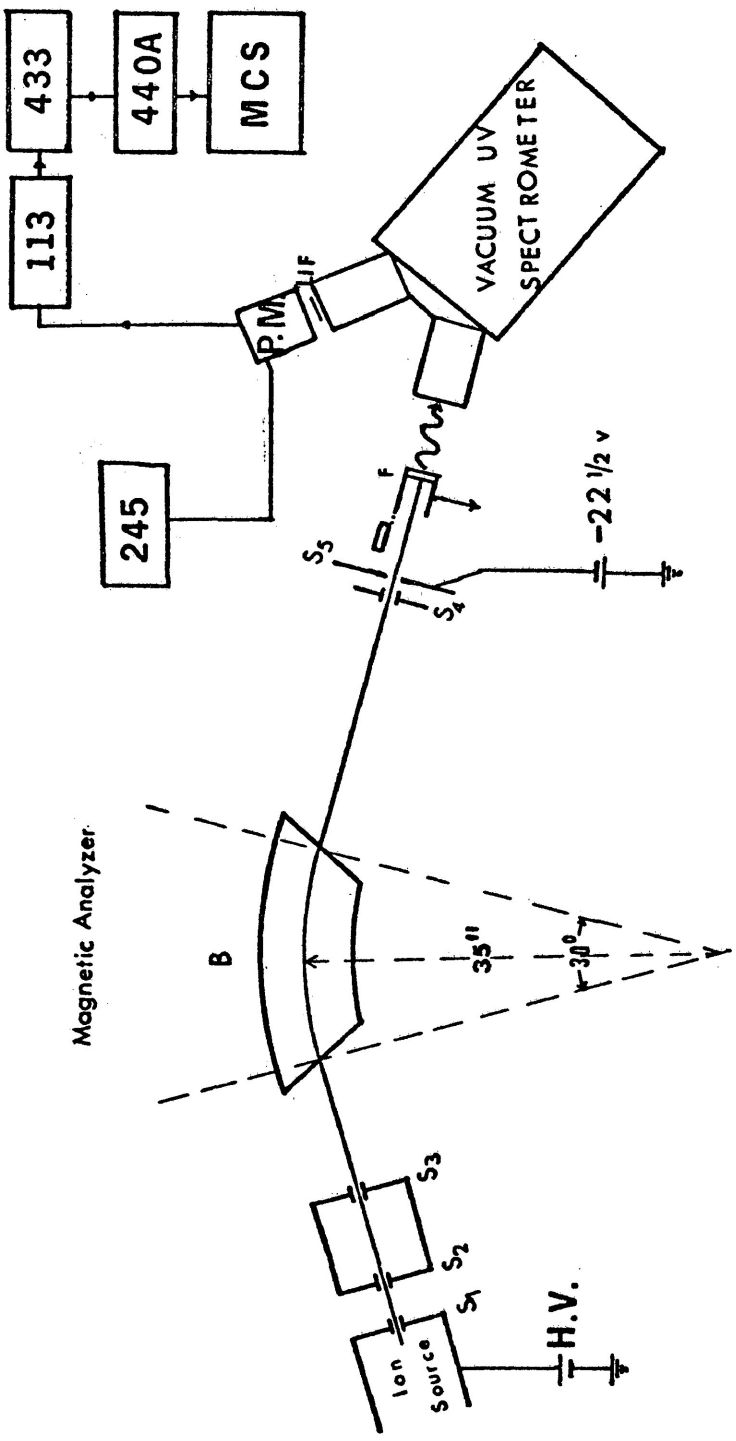

Fig. 6. Schematic diagram of apparatus.

violet scanning spectrometer was aligned with the direction of the ion beam. The luminescence spectra were detected by an EMI type 9365A photomultiplier at the exit slit after passing through a LiF window. As the luminescent response was rather low for ion excitation, as compared with that of ultra-violet excitation, both the entrance and exit slits were set wide open at 1.5 mm. To detect this still low scintillation response, the photomultiplier output was passed through an Ortec model 113 preamplifier, an Ortec model 433 sum-invert amplifier, and Ortec model 440A selectable active filter amplifier (coarse gain HI 64, fine gain 10.00, shaping time 1 μsec.). The output pulses were then fed into a Hewlett-Packard 5400A multi-channel analyzer operated in the multi-channel scaling mode. The digital readout from the memory was printed out by Teletype and punched tapes were also obtained.

While the whole system was pumped down and maintained in the range of $1.0 - 10 \times 10^{-6}$ torr with a selected gas leaking in, the accelerator was adjusted to give the desired ion beam at the desired ion energy. The ion current was then measured and the luminophor sample moved into the beam. Each channel of the multi-channel scaler accumulated the pulse count associated with the scintillation response for a certain wavelength interval. Initially the spectrometer was set so that by the time the multi-channel scaler was at the middle of the time interval for channel number one, the spectrometer indicated the starting wavelength of the luminescent spectrum observed. Both the spectrometer scanning and the multi-channel sweeping were started at the same time. Thus each channel, except channel number zero, registered

the total pulse count corresponding to a consecutive wavelength interval. This count number, after the background count for the dark current of the photomultiplier was deducted, was taken as the measure of the average count for the wavelength reading at the middle of the wavelength interval of its associated channel. The maximum count for a sweep of the multi-channel scaler varied with ion energy, ion current and, most probably, other factors. It varied from a few hundreds to a few ten thousands. The background current was 135 counts/channel on average. Thus those spectra with a few hundreds as their maximum count were rejected and only those with higher maximum counts were used to ascertain their peak positions, the relative peak intensities and the bandwidths. The ion current was re-measured at the end of the sweeping of the multi-channel scaler.

As the arrangement suffered from the fact that the ion current could not be monitored while a spectrum was being run, a more sophisticated target chamber was built to couple the ultra-violet spectrometer and the ion accelerator which allowed the simultaneous measurement of both the spectrum and the light emitted from the sample. As shown in Fig. 7, a rotary holder in the target chamber was utilized to attach the samples, five at a time. The rotary holder could be moved horizontally by a rotary bellows feedthrough and a rack and pinion system. If the rotary holder was moved to one of its extreme positions, it could be rotated through an angle of 72°. While it was moved to the other far end, the Faraday cup was moved in the direction of the ion beam and hence the ion current could be measured. After passing through the slits, the ion beam struck the sample S (see also

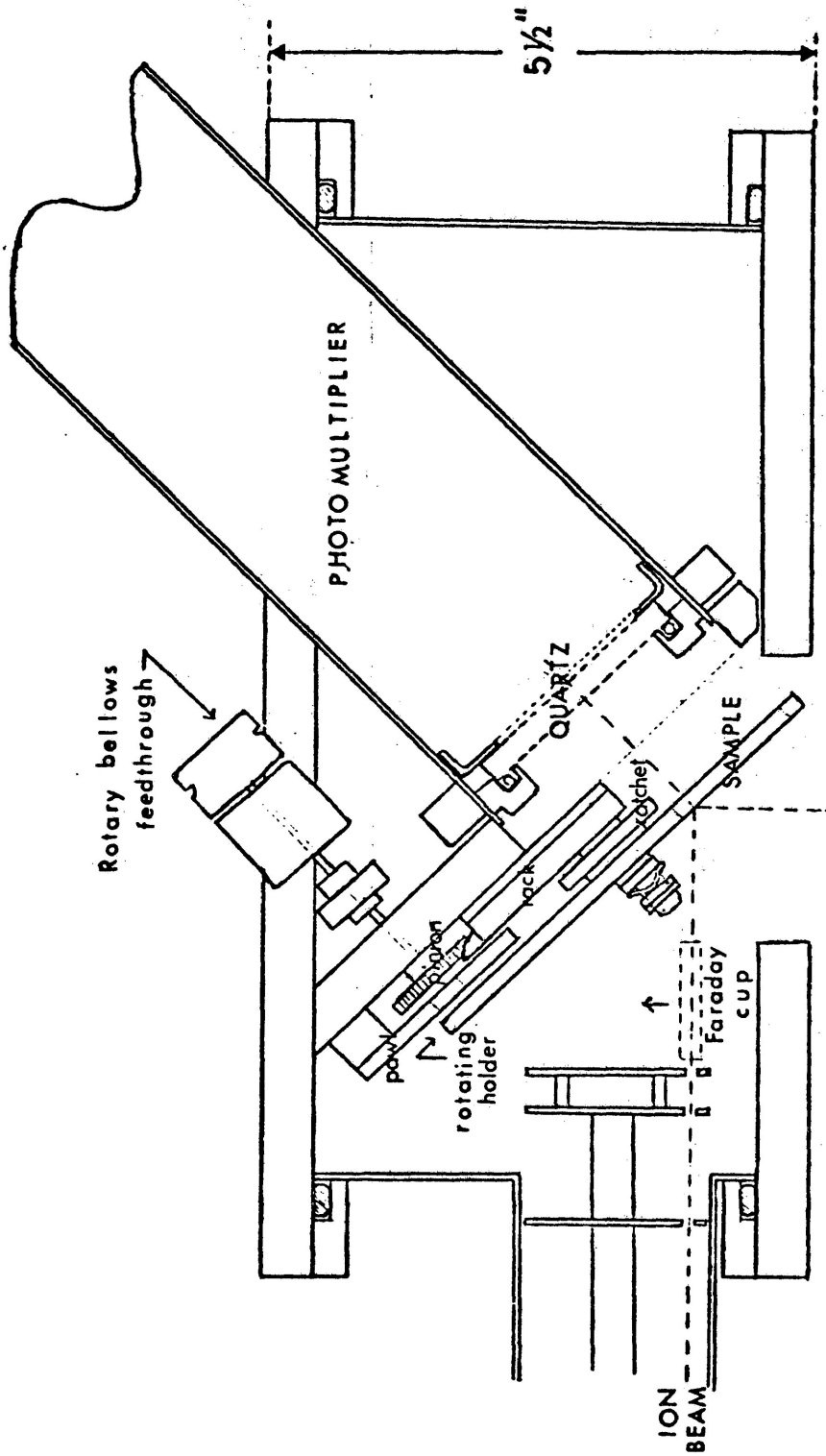

Fig. 7. The second target chamber approximately to scale.

Fig. 8) at an angle of 45° to its surface and irradiated an area of .1 cm × 1.06 cm. The light produced entered the spectrometer directly without passing through either the sample or the quartz plate. The quartz discs used to hold the sample were coated with thin, partially reflecting, aluminum films to prevent the sample from charging up during ion bombardment. A low dark current photomultiplier, P in Fig. 8, (EMI type 9502SA) was selected to monitor the light produced which was transmitted through the sample. A Keithley type 246 power supply operated at -1000V was used as the high voltage supply. The output was passed through a Keithley 410A Picoammeter and was recorded by a Bausch and Lomb type V.O.M.5 chart recorder. Other parts of the apparatus arrangement were the same as those set up for the first arrangement, except an Ortec model 408 biased amplifier was used instead of the 433 sum-invert amplifier so that the bias voltage could be adjusted to get the best signal-to-noise ratio. The output of the 245 High Voltage Supply was -1100V. A Hewlett-Packard 7005B X-Y Recorder was used to plot the spectra from the memory of the multi-channel scaler.

The second arrangement was far superior to the original one in that it allowed the spectrometer to look directly at the light produced by the sample and thus in the future could be used to extend measurements into the vacuum ultra-violet. It also allowed the direct monitoring of the ion integrated response of the luminophor. The target chamber was maintained at a pressure of $1 - 2 \times 10^{-7}$ torr by means of a HVEC model FPS-800, 4 in. diffusion pump with a liquid nitrogen baffle.

The procedure adopted in obtaining data was mainly the same as that for the preliminary experiment. While the ion beam was bombarding

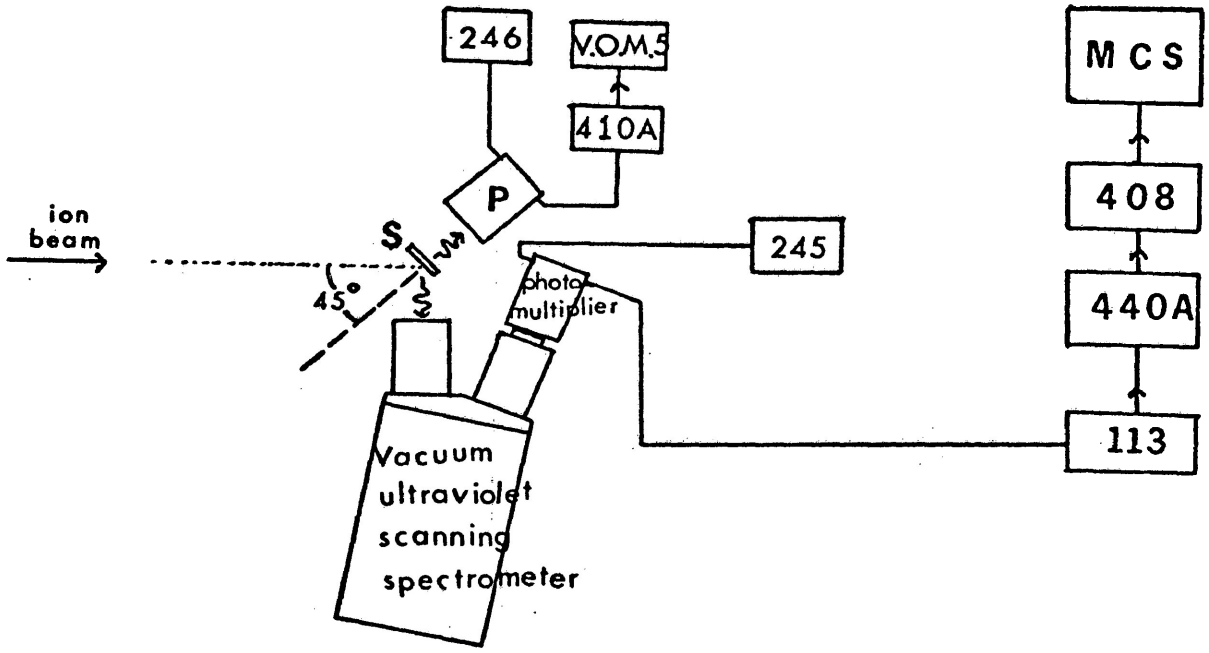

Fig. 8. Schematic diagram of apparatus.

the luminophor, the light L produced by the sample was monitored and repetitive scans of the luminescent spectrum were made. After a sufficient number of scans was made, the sample was removed from the beam and the current re-measured. The accelerator itself was fairly stable and capable of maintaining a relatively steady current for periods of several hours. If the accelerating voltage did drift or the current varied for some other reason in a run, it was immediately obvious on the recorder tracing of the light produced by the sample. Usually the current could be restored by adjusting the accelerating potential slightly.

V

RESULTS

Spectral Distribution of Luminophors Under Ultra-Violet and Ion Excitation

Samples of the various luminophors were irradiated with 2537 Å, 3130 Å and 3650 Å ultra-violet light and luminescent spectra recorded. Similar samples were exposed to beams of $^{1}H^{+}$, $^{4}He^{+}$, $^{14}N^{+}$, $^{20}Ne^{+}$ and $^{40}Ar^{+}$ and the spectra of the transmitted light recorded. For each ion about 10 spectra were taken each at a different energy in the energy range from 10 - 100 KeV. During these runs, the ion current was kept as low as possible to prevent deterioration of the sample. It was, however, necessary to keep this lower limit fairly high in order to obtain reasonable spectra. Thus for heavy ions and easily damaged luminophors such as *ZnS:Ag* a considerable amount of damage is certain to have occurred. It was thought originally that the damage would have little influence on the ionoluminescent spectra obtained.

Table I presents the data obtained from this part of the experiment. The first column indicates the luminophors and their JEDEC number. The second column indicates the photon energy at the peak, the standard error associated with it and the number of spectra obtained, in that order, for ultra-violet 2537 Å irradiation. The number immediately below the peak energy is the bandwidth at half maximum in electron volts. The third and fourth columns give the corresponding numbers for ultra-violet 3130 Å and 3650 Å excitation, respectively. Those peak energies given without the standard errors were obtained each

TABLE I

Emission peaks and bandwidths observed for various luminophors under ultra-violet and ion excitation.

(Units except for numbers in parentheses are electron volts)

	λ = 2537 Å	λ = 3130 Å	λ = 3650 Å	H^+	He^+	N^+	Ne^+	Ar^+
P - 1 $Zn_2SiO_4:Mn$	2.384 ± 0.0009(9) 0.16	very weak	no emission	2.38 0.16	2.38 0.16	2.38 0.16	2.38 0.15	2.38 0.15
P - 2 $ZnS:Ag:Cu$	2.438 ± 0.0012(24) 2.774 ± 0.0050(7) 0.63	2.441 ± 0.0010(13) 2.76 0.64	2.441 ± 0.0010(17) 2.78 0.64	2.46 2.80 0.66	2.46 2.81 0.67	2.46 2.80 0.67	2.46 2.82 0.67	2.45 2.82 0.66
P - 5 $CaWO_4$	3.01 0.72	no emission	no emission	3.01 0.71	3.02 0.61	3.00 0.71	2.98 0.71	3.01 0.71
P-11 $ZnS:Ag$	2.772 ± 0.0013(9) 0.35	2.76 0.33	2.77 0.32	2.77 0.35	2.77 0.36	2.78 0.35	2.77 0.36	2.77 0.35
P-20 $ZnCdS:Ag$	2.36 0.28	2.36 0.27	2.36 0.27	2.38 0.29	——	2.37 0.29	2.38 0.31	2.38 0.27
P-22 $ZnS:Ag$	2.779 ± 0.0014(12) 0.31	2.77 0.31	2.77 0.31	2.78 0.33	2.79 0.34	2.79 0.34	2.78 0.31	——
P-22 $ZnCdS:Ag$	2.39 0.28	2.39 0.28	2.39 0.28	2.41 0.30	2.41 0.31	2.40 0.28	2.39 0.28	2.41 0.29
P-31 $ZnS:Ag:Cu$	2.391 ± 0.0016(4) 2.708 ± 0.0048(4) 0.59	2.38 2.69 0.60	2.39 2.71 0.60	2.40 2.74 0.49	2.38 2.74 0.50	——	2.39 2.71 0.47	——

from single spectra. The other columns give the corresponding numbers for H^+, He^+, N^+, Ne^+ and Ar^+ excitation. Each value of these numbers was obtained as the average value of about ten spectra excited at different energies. The uncertainty is estimated to be a few tenths of an electron volt. Two peaks were obtained for each *ZnS:Ag:Cu* luminophor. Their bandwidths were taken as the difference in energies between the positions corresponding to the left half maximum of the left peak and the right half maximum of the right peak.

Fig. 9 illustrates the spectra recorded for *ZnS:Ag:Cu* (P-2) luminophor excited by the three different ultra-violet wavelengths. These curves, which are typical of those obtained for *ZnS* type luminophors, are normalized at the green peak. The luminescent response varies rather slowly around the luminescent peaks. In addition to this, the irregular fluctuation of the luminescent response superimposed on the whole broad band profile makes the peak position uncertain to the extent of 0.01 eV though the accuracy of the spectrometer allows the determination of wavelength to within ± 1 Å (~ 0.002 eV). The presence of two broad overlapping bands of comparable intensities also makes it difficult to determine the correct positions of the luminescent peaks.

It is to be noted that there appears to be little different between the peak energies of samples excited by ions and those excited by ultra-violet light. The *ZnS* type luminophors showed slight displacement which may or may not be significant. It was these slight differences which led to the more thorough investigation of the *ZnS:Ag:Cu* luminophor.

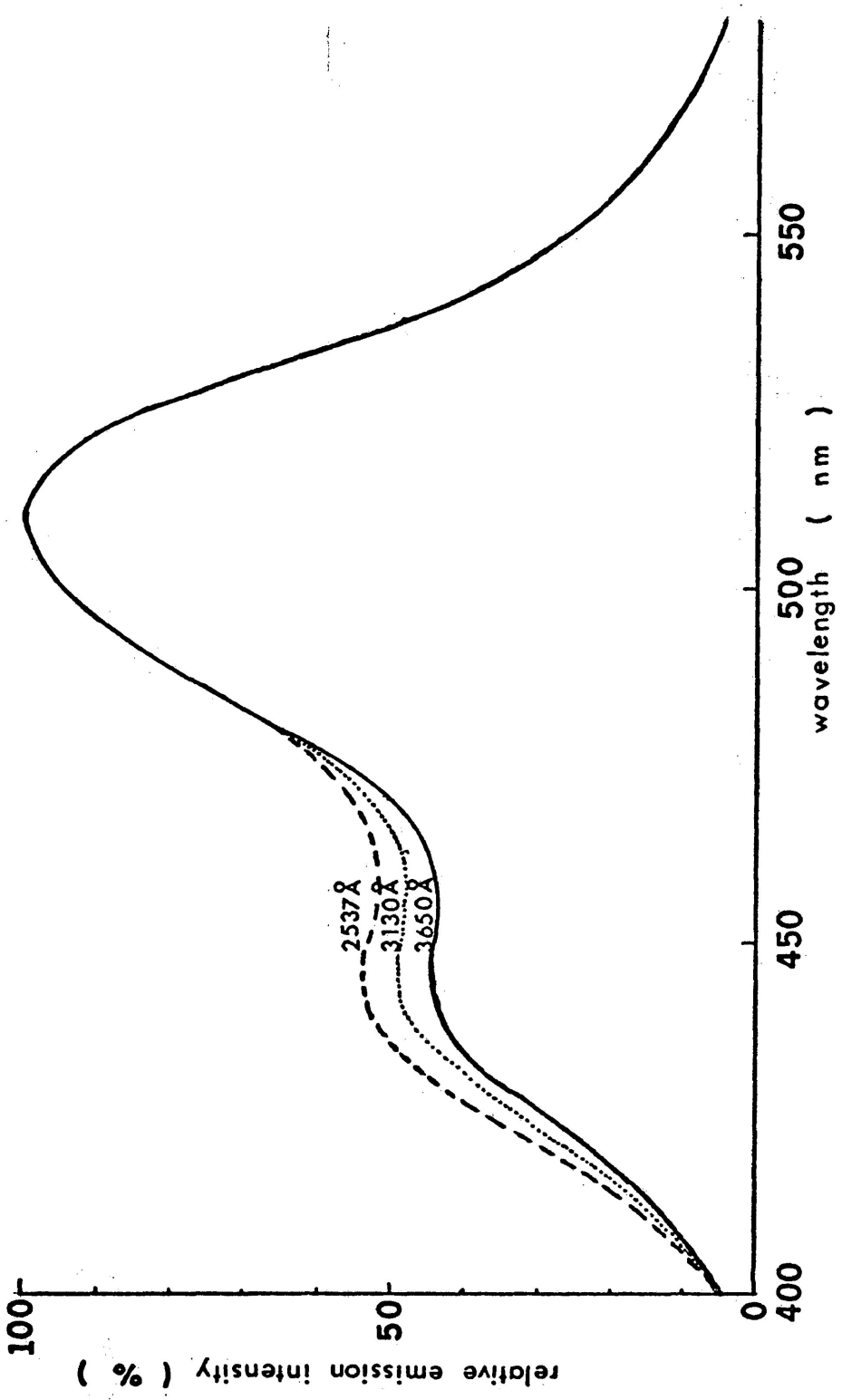

Fig. 9. Luminescent spectra of *ZnS:Ag:Cu* (P-2) excited by 2537 Å, 3130 Å and 3650 Å ultraviolet light at room temperature.

Ionoluminescence Spectra of *ZnS:Ag:Cu* (P-2)

It is known that the photoluminescent spectrum of *ZnS:Ag:Cu* consists of a blue *Ag* emission band partially overlapping with a green *Cu* emission band.[28] The luminophor was prepared with chloride fluxes and thus it is chlorine coactivated.[29] Shionoya *et al.*[21] asserted that the *Ag*-blue emission is due to the pair-emission of the *Ag* acceptor and the *Cl* donor, while *Cu*-green emission is due to that of the *Cu* acceptor and the *Cl* donor. The ionoluminescence produces a blue peak with an energy of about 2.81 eV and a green peak of about 2.46 eV. Although the energies of the peaks did not appear to change significantly with ion energy or mass, it was noted that the relative intensity of the two peaks seemed to change erratically as data were obtained. This was initially thought to be due to changes in the efficiency of the luminophor during a spectral scan due to deterioration of the sample or fluctuation in the beam current. In order to overcome such difficulties, the second target chamber described in the previous section was constructed. As was indicated, this chamber allowed the simultaneous determination of the integrated light output of the sample, as well as the spectral distribution of the luminescence. This allowed the normalization of the spectral distribution curves to take into account changes in the total amount of light being produced.

Fig. 10 is an illustration of the data obtained during a run with Ne^{++} at 100 KeV. The top curve corresponds to the recorder tracing of the integrated light output as a function of time. It is to be noted that the light output decreases fairly rapidly. This decrease in

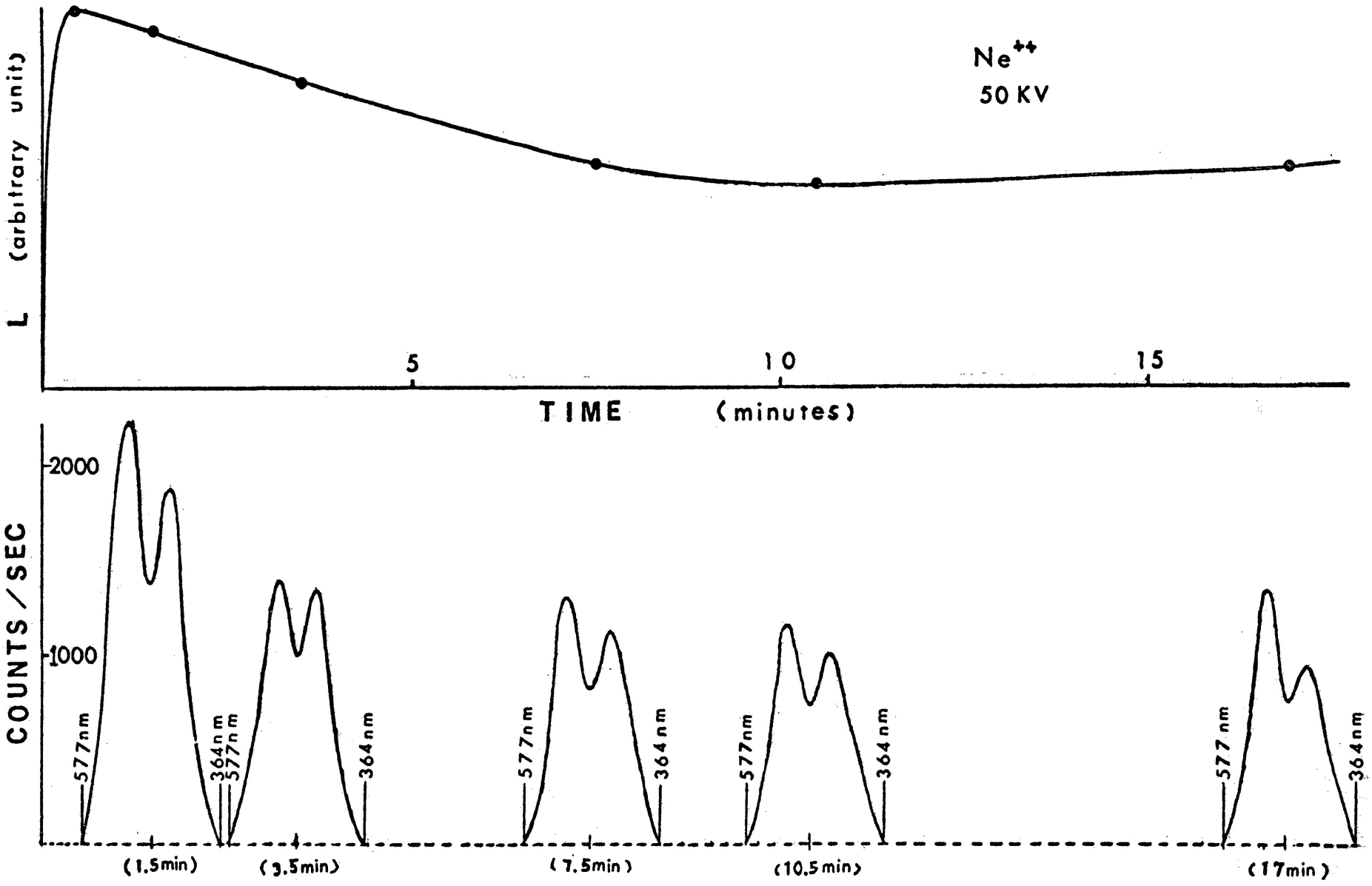

Fig. 10. Deterioration curve and ionoluminescent spectra of *ZnS:Ag:Cu* (P-2) under Ne^{++} 50 KeV excitation at room temperature.

light output was due to the deterioration of the sample by the incident ions. This deterioration could not be avoided since a fairly high current density ($\sim 10^{-9}$ amp/cm^2) was necessary to produce enough light to obtain a reasonable spectrum. The lower curves in the figure are the spectra recorded approximately at the times corresponding to the adjacent points in the upper curve. As we move to the right, each spectrum is produced by the same sample which has received a larger dose of ions than it had in the preceding spectrum. It is to be noted that the area under the spectral peaks decreases as the total amount of light decreases.

Fig. 11 is a plot of L/L_0 *versus* D, the total ion dose for H^+ where L_0 is the initial integrated light output. It is to be noted that the luminophor deteriorates more rapidly under bombardment with low energy hydrogen than with high energy hydrogen. The behavior is well understood and is due to the fact that the nuclear stopping cross section is large only at low energy (~ 5 KeV).[24] The actual form of these curves is very difficult to predict since the rate at which the H^+ ion does damage varies along the path of the ion[22] as does the light produced. At high energies, the light output grows. This anomalous behavior is shown for the curves for 50 KV, 70 KV and 84 KV H^+ ions.

Fig. 12 and Fig. 13 are plots of L/L_0 *versus* D for Ne^+. Here it is to be noted that the rate of deterioration increased with energy. This is also well understood since the rate at which *Ne* does damage, which is proportional to S_n, increases with ion energy over a large portion of the energy range studied. For very low energy, however, Ne^+ behaves quite anomalously and the efficiency of the luminophor increases rather than decreases. This feature was observed for N_2^+, Ar^+ and Ar^{++} at low

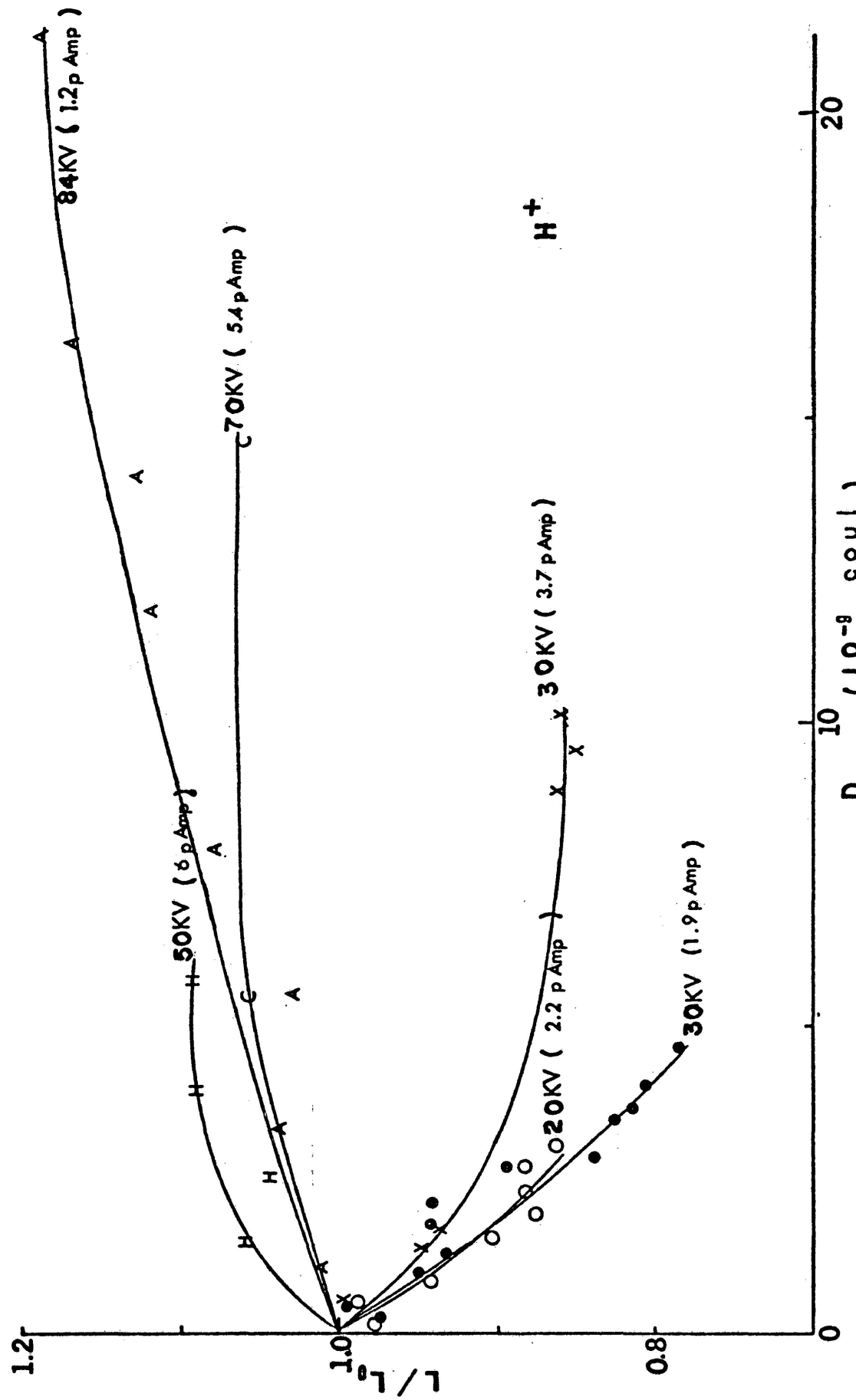

Fig. 11. Integrated light output *versus* ion dose for H^+ ions incident on *ZnS:Ag:Cu* (P – 2) luminophors.

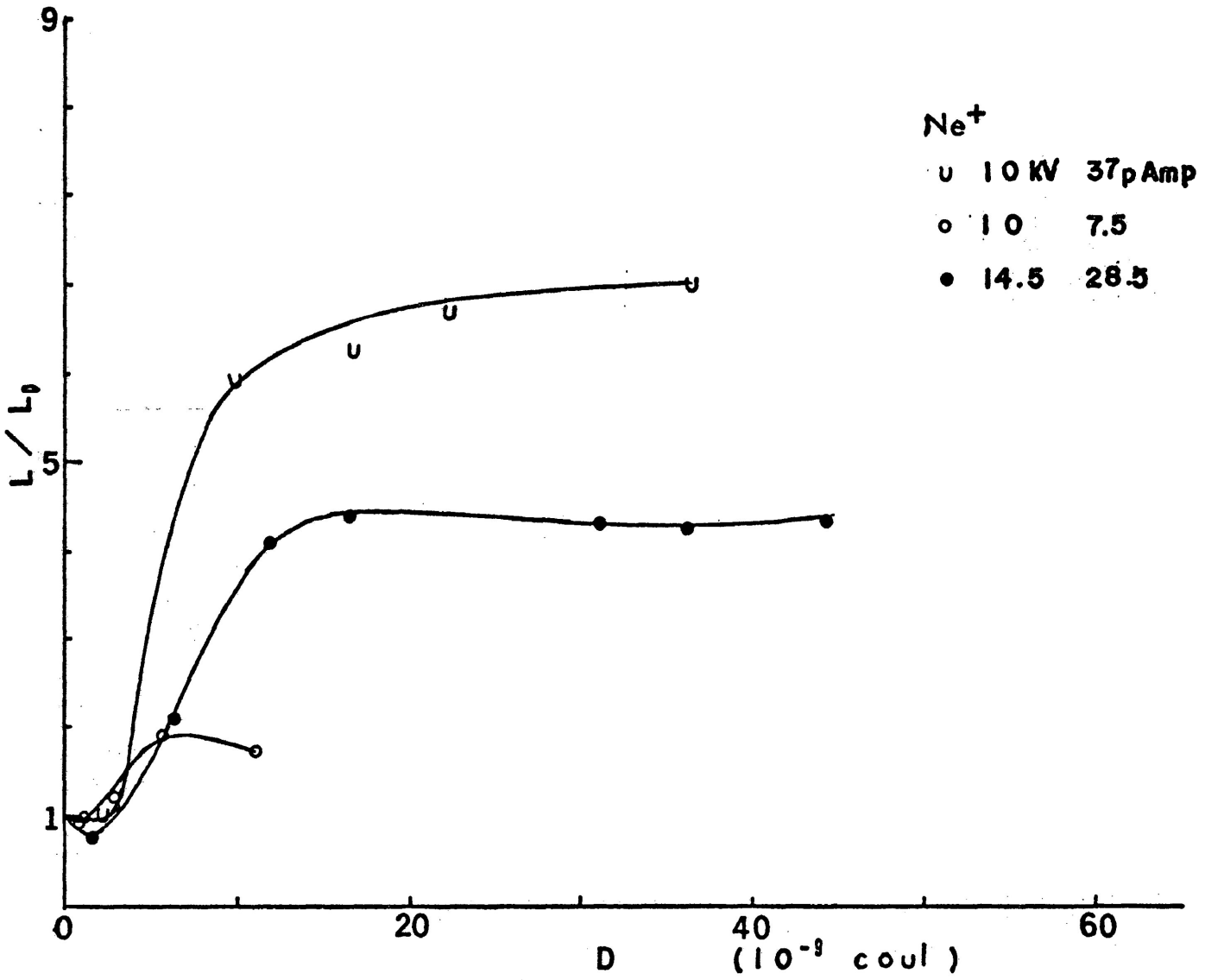

Fig. 12. Integrated light output *versus* ion dose for Ne^+ ions incident on *ZnS:Ag:Cu* (P-2) luminophors.

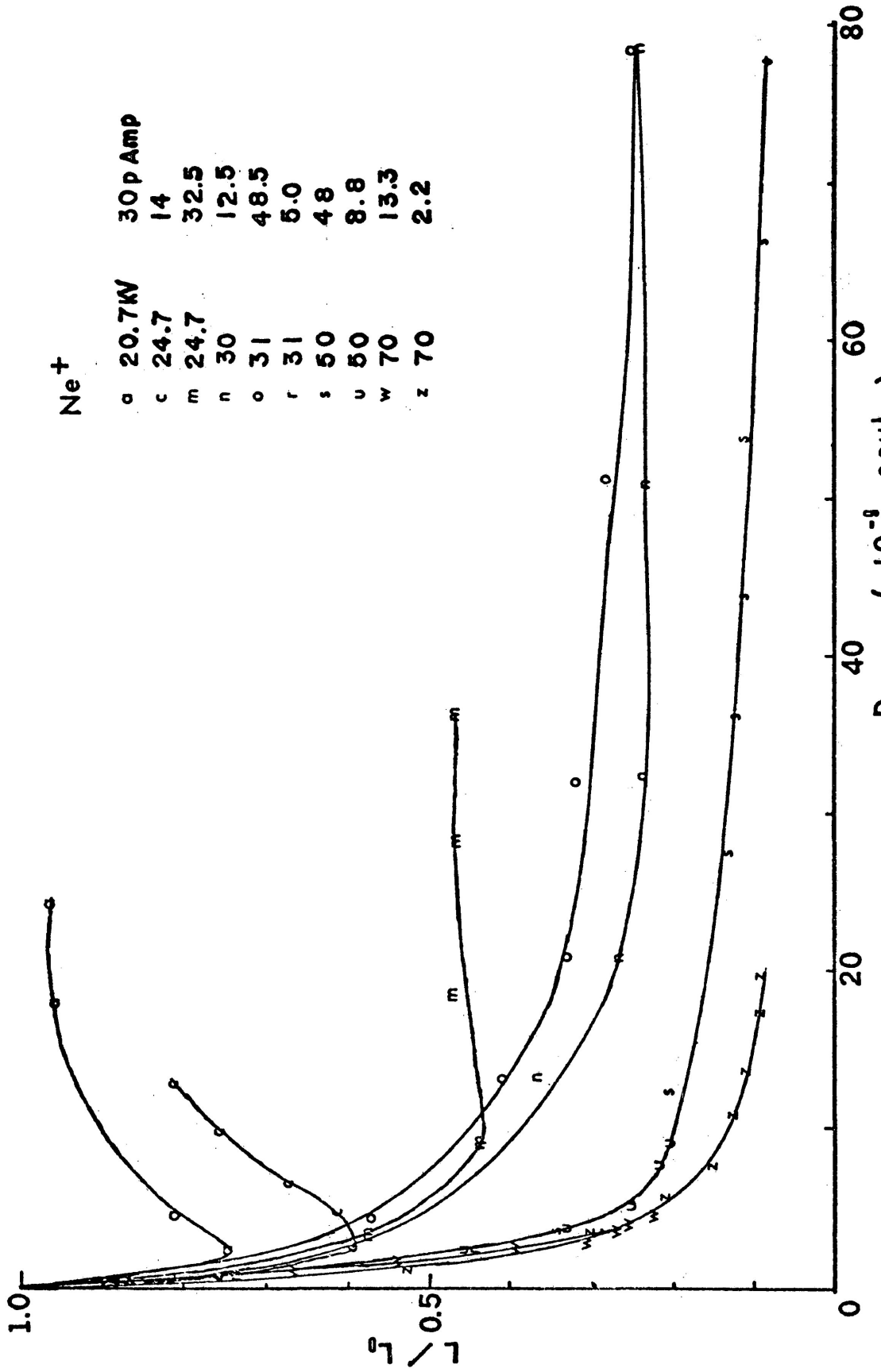

Fig. 13. Integrated light output *versus* ion dose for Ne^+ ions incident on *ZnS:Ag:Cu* (P-2) luminophors.

energies as well. A tentative explanation for this behavior will be discussed in the next section. The present experiment was not designed to determine accurately the rate of deterioration. Slight changes in beam direction caused the beam to impinge upon fresh portions of the sample and thus after a particular portion of the luminophor had been subjected to a large dosage and L/L_0 reduced to about 0.1, the light output L tended to become rather unsteady. This led to considerable uncertainty in the value of L/L_0 for large doses.

Fig. 14 is a semi-log plot of $D_{1/2}$, the dose required to reduce the light output by a factor of 2 (i.e., $L_0/L = 2$) *versus* ion energy. For H_2^+ and N_2^+, the points were obtained by considering the molecular ion with an incident E to be equivalent to two monoatomic ions each with an energy of $E/2$. A smooth curve may be drawn through the points obtained using N^+ and N_2^+ and also through the points obtained using Ne^+ and Ne^{++}. It is thus believed that as far as the deterioration of the luminophor is concerned the charge state of the incident projectile is not critical. The magnitudes of $D_{1/2}$ for the various ions are also as one would expect. S_n increases as the ion mass increases. Thus the number of ions required to produce a given amount of damage decreases as the mass increases. The shapes of the curves are also in qualitative agreement with theoretical predictions. Since S_n decreases with energy in the range of energies studied for H and He, $D_{1/2}$ increases. For N and Ne, S_n has a maximum in this energy range, thus $D_{1/2}$ increases at high energies. S_n for Ar increases over almost the entire range, thus $D_{1/2}$ decreases with energy.

Fig. 15 is a semi-log plot of R, the ratio of the emission in-

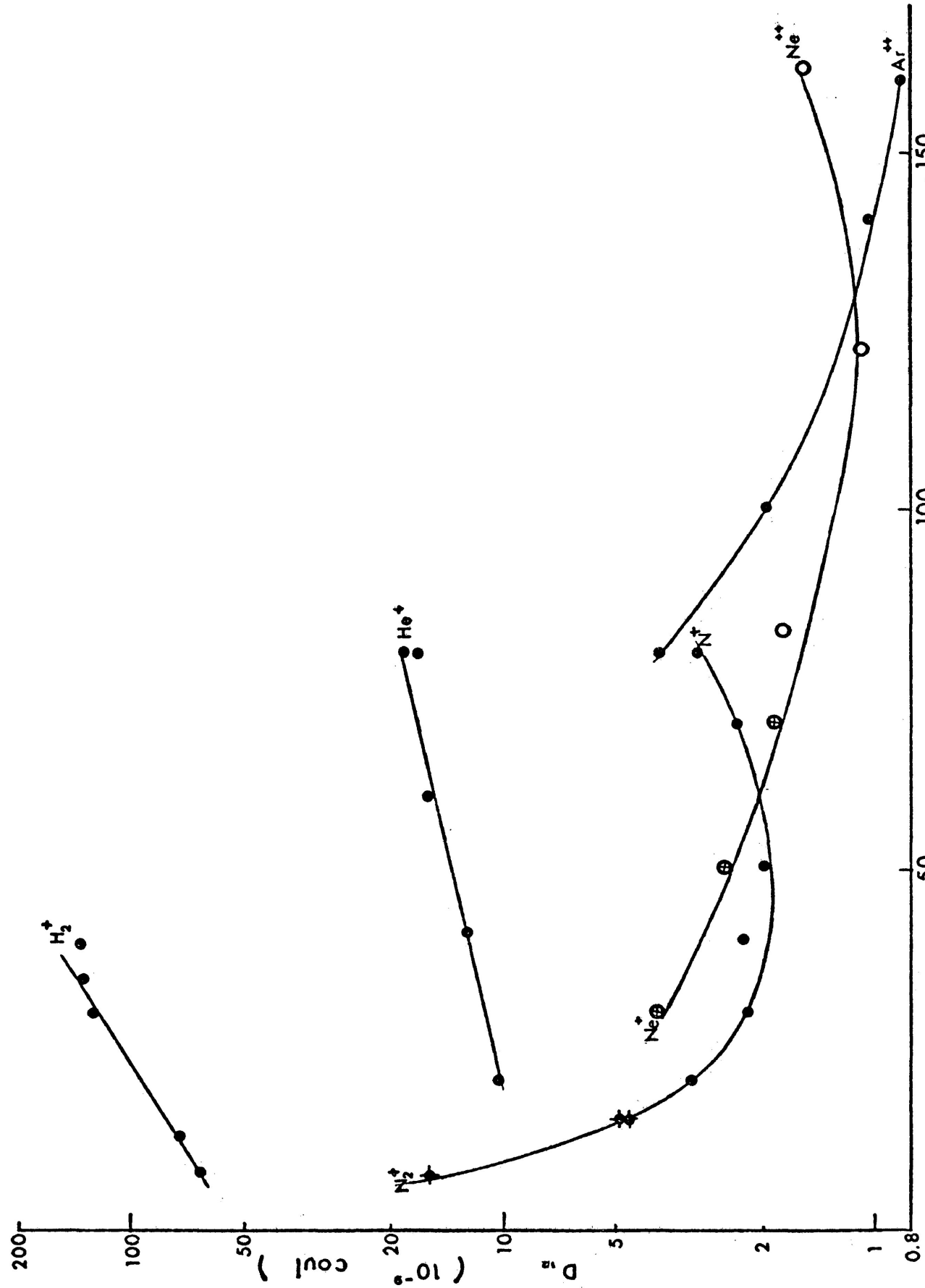

Fig. 14. Doses required to reduce the light output by a factor of 2 *versus* ion energy for *ZnS:Ag:Cu* (P-2).

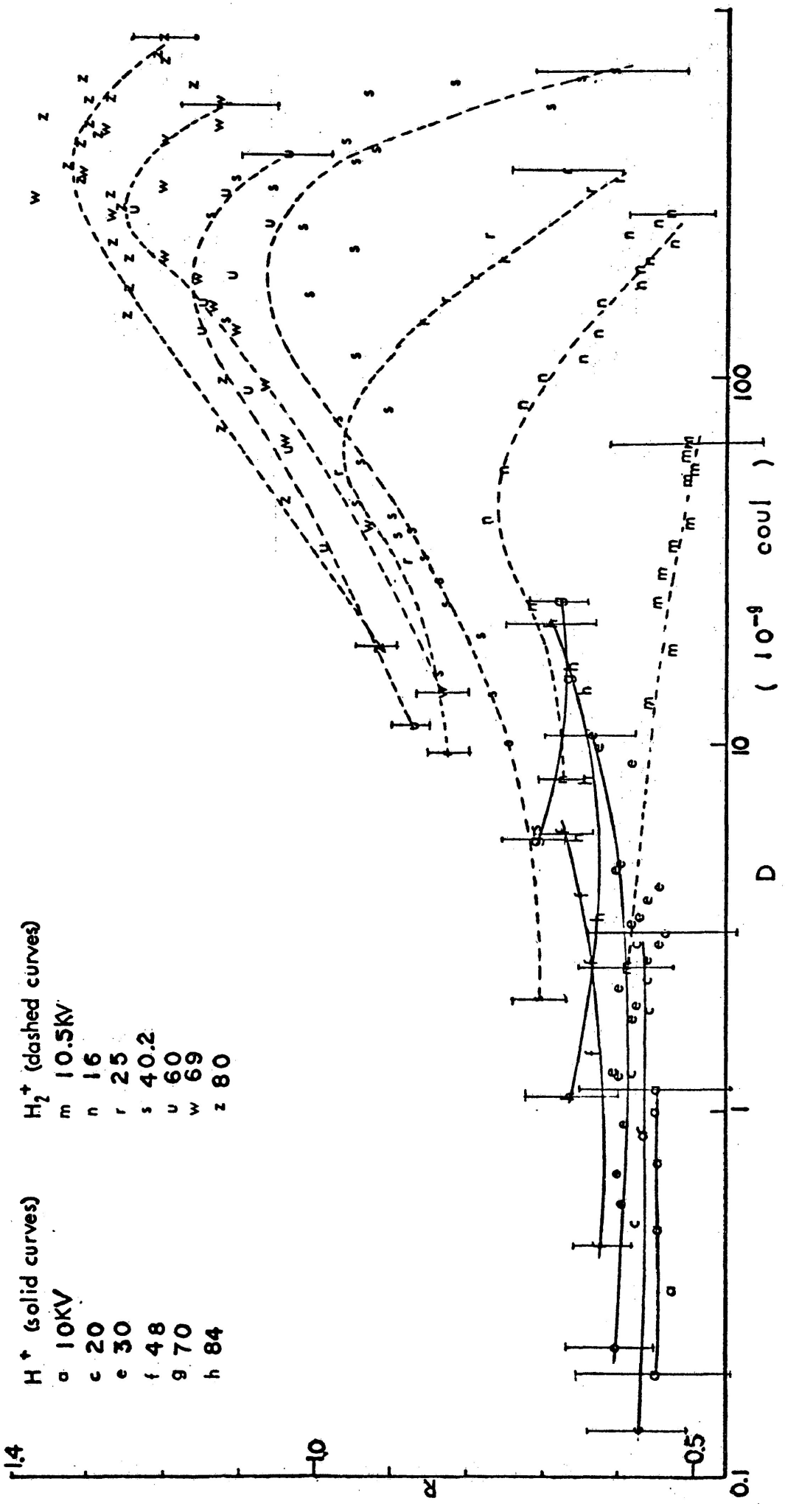

Fig. 15. Ratio of peak heights *versus* ion dose for hydrogen incident on *ZnS:Ag:Cu* (P-2).

tensity of the blue peak to the emission intensity of the green peak for hydrogen incident on *ZnS:Ag:Cu* (P-2) *versus* the average ion dose during the scanning of the spectrum. These intensities were obtained from a recording of the multi-channel scaler output from which background counts were subtracted. The peak intensities were normalized according to the value of L while they were being scanned. Each curve corresponds to the indicated ion energy. The D value for H_2^+ is taken as twice the monoatomic ion dose. The scattering in the points for large D is due to the fact that the integrated light output after a large dose is small and fluctuations in the background make the exact determination of the peak height impossible. Error bars at the extremes of the curves indicate estimated uncertainties. Unfortunately, it was impossible to achieve high currents with H^+ and thus there is little overlap between the H^+ regions and the H_2^+ regions of the figure. Comparison of the 60 KV H_2^+ with the 30 KV H^+ indicates that these ions behave considerably differently even though one might expect the opposite. The discrepancy between points obtained using 40 KV H_2^+ and 80 KV H^+ is also quite large. These curves do, however, exhibit some general features. At low doses, R is of the order of 0.5 to 0.7. As the dose is increased, R reaches a maximum, R_{max}, which varies from about 0.75 for H_2^+ at 16 KV to about 1.3 for H_2^+ at 80 KV. The dose at which the maximum occurs increases with increasing ion energy.

Fig. 16 is a similar plot for He^+. Again it was difficult to obtain high enough currents to attain large doses in reasonable lengths of time. The only curve which shows signs of a maximum is that obtained at the lowest energy. It appears that the other curves might have maxima at

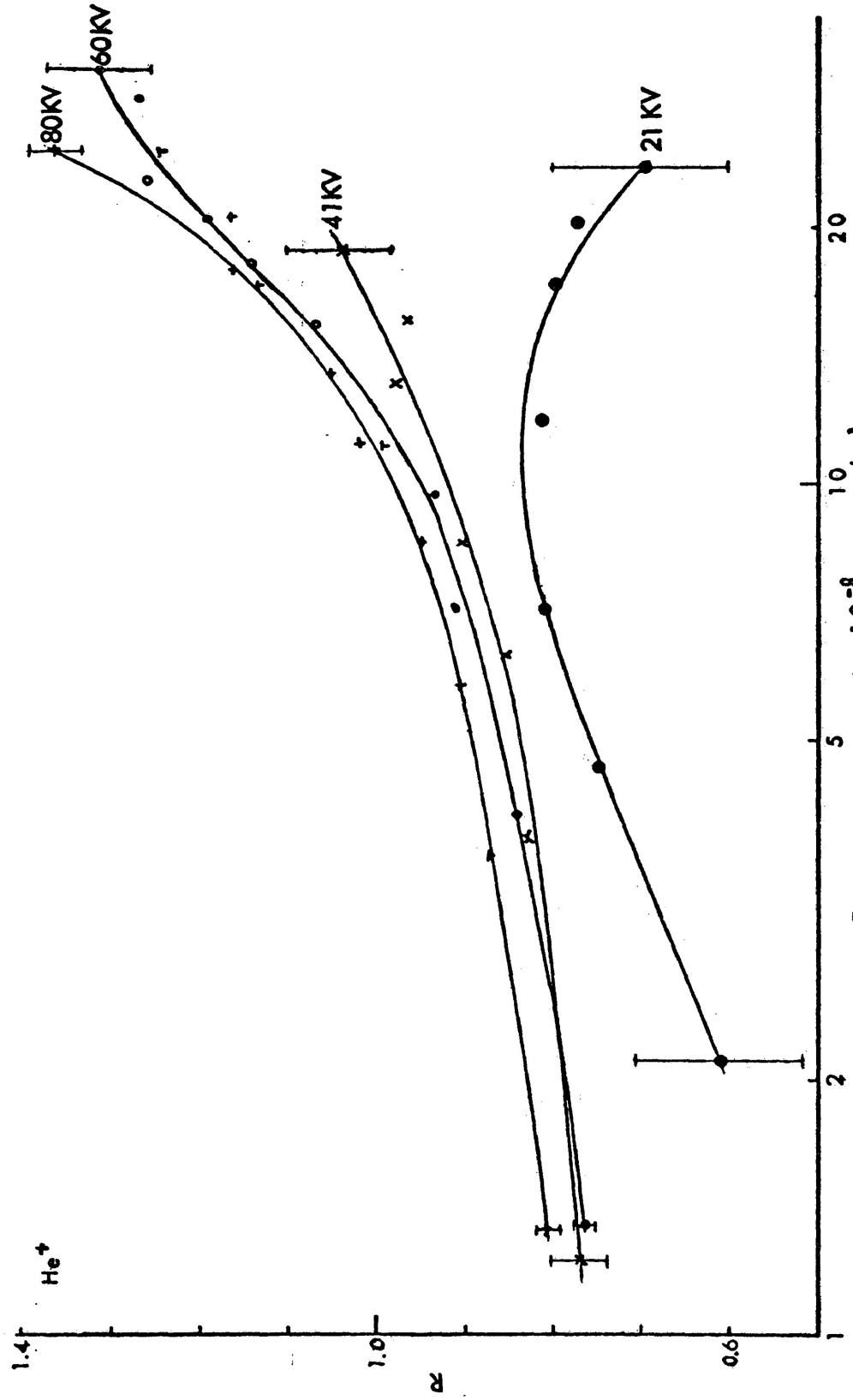

Fig. 16. Ratio of peak heights *versus* ion dose for helium incident on *ZnS:Ag:Cu* (P-2).

higher doses. R tends to increase with ion energy.

Fig. 17 is a semi-log plot of R *versus* D obtained using nitrogen. The solid curves were obtained using N^+ and the dashed curves N_2^+. It can be seen that there is a considerable variation in R_{max} which has a value of about 0.5 for N_2^+ at 15 KV and about 1.3 for N^+ at 80 KV. The curves obtained for equivalent pairs of N^+ and N_2^+ do not agree at all well as was the case with H^+ and H_2^+. It appears that the molecular ion produces a higher value for R than the monoatomic one. The dose at which R_{max} occurs does not appear to change with ion energy nearly as much as for H_2^+.

Fig. 18 is a similar plot for neon. The solid curves were obtained using Ne^+ and the dashed curves Ne^{++}. R_{max} varies from about 0.4 for Ne^+ at 30 KV to about 1.25 for Ne^{++} at 80 KV. R appears to increase for increasing ion energy. The dose at which R_{max} occurs scatters around $1 - 3 \times 10^{-9}$ coul.

Fig. 19 is a semi-log plot of R *versus* D for argon. R_{max} appears to increase with energy. The dose at which R_{max} occurs does not change much with respect to the ion energy. The value of R_{max} varies from about 0.45 for Ar^+ at 15 KV to about 1.2 for Ar^{++} at 80 KV.

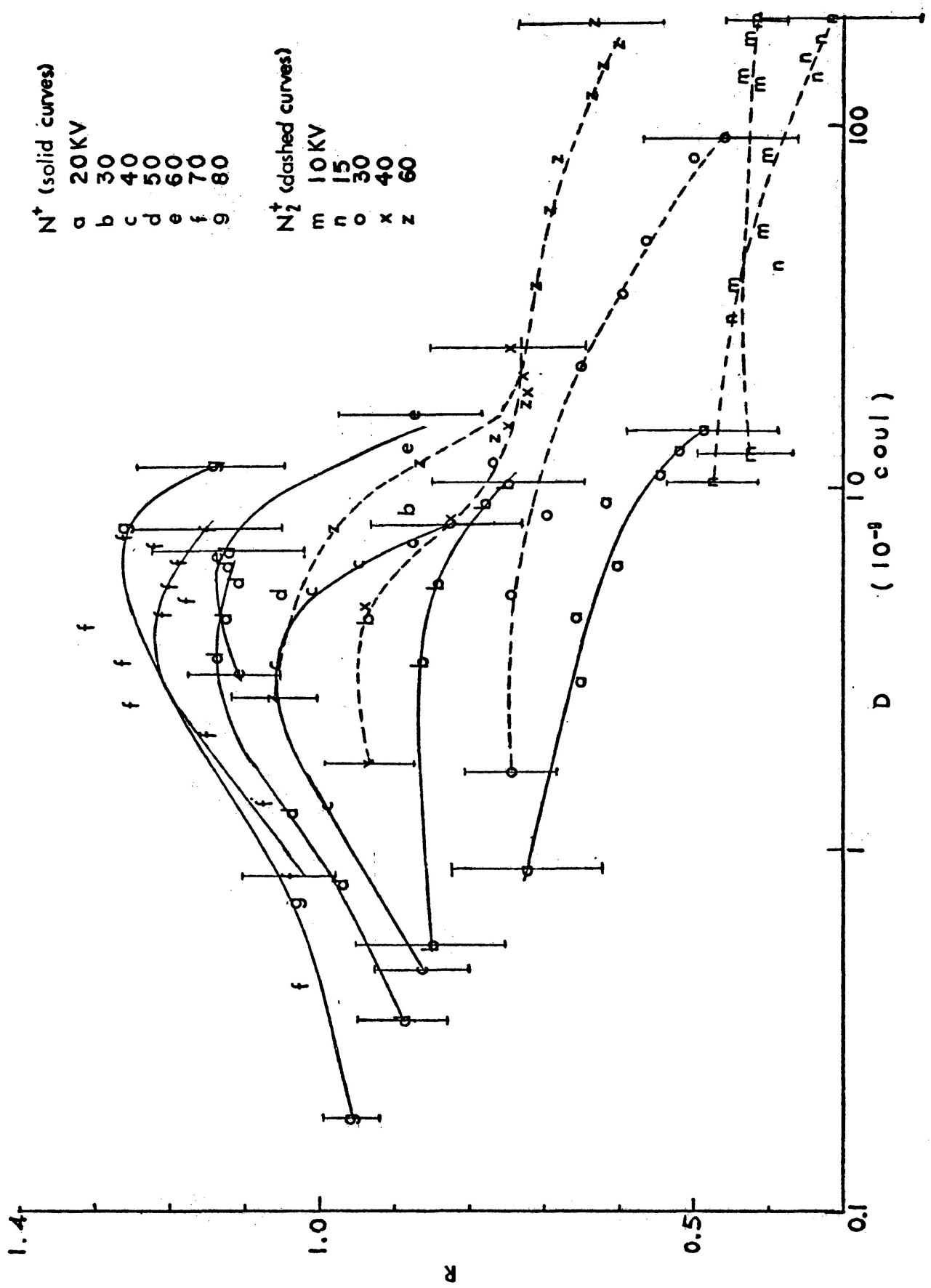

Fig. 17. Ratio of peak heights *versus* ion dose for nitrogen incident on *ZnS:Ag:Cu* (P-2).

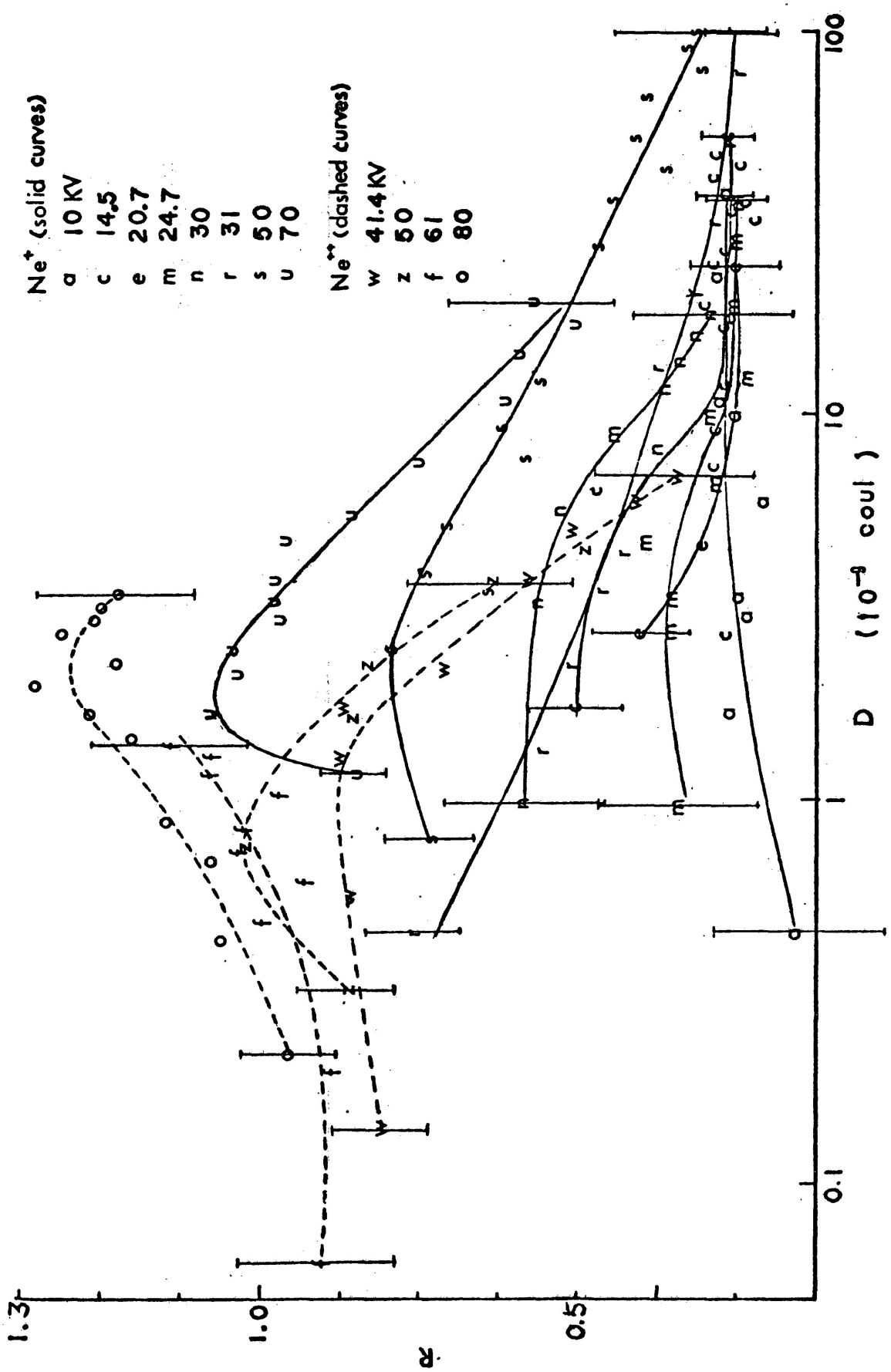

Fig. 18. Ratio of peak heights *versus* ion dose for neon incident on *ZnS:Ag:Cu* (P-2).

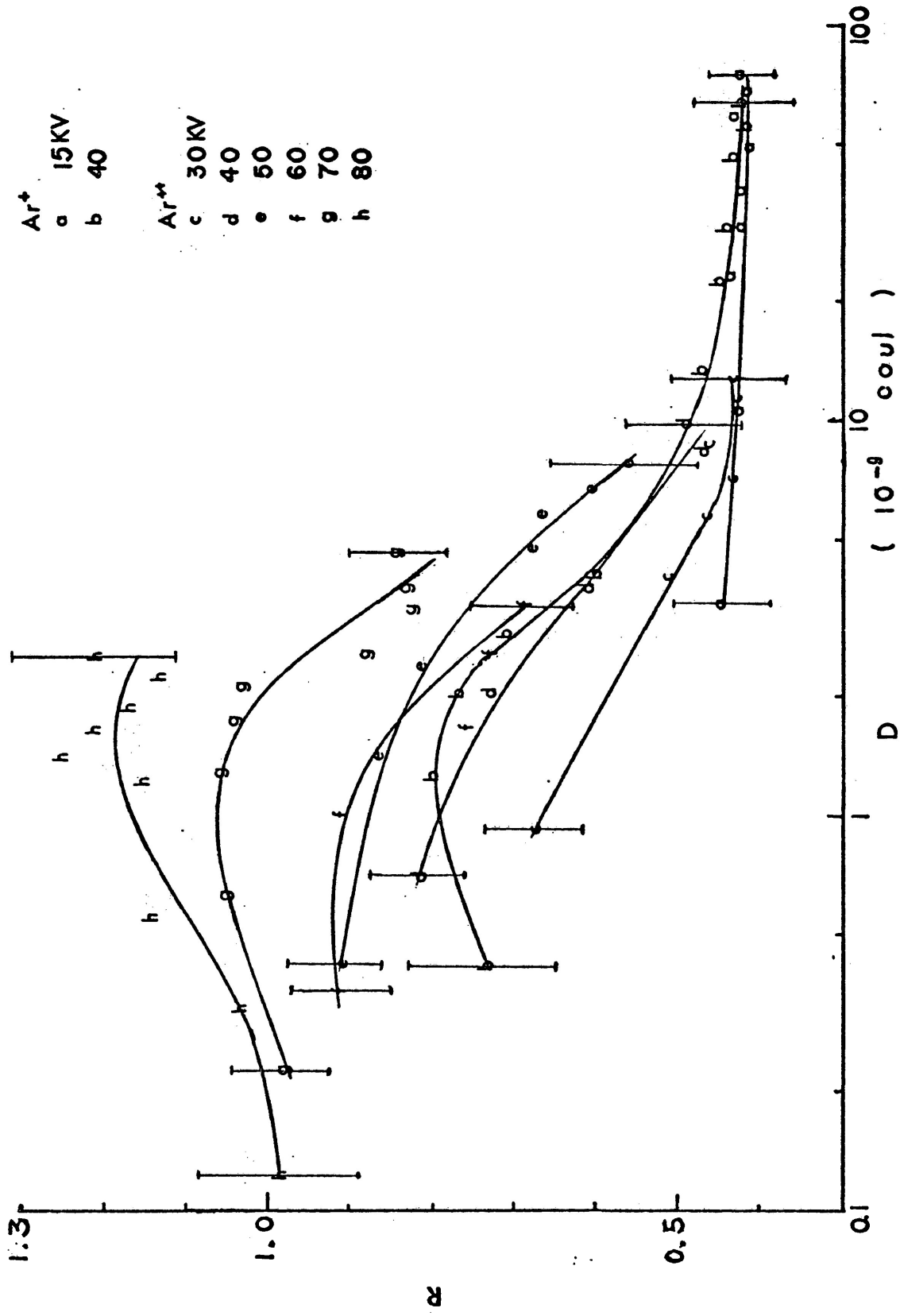

Fig. 19. Ratio of peak heights *versus* ion dose for argon incident on *ZnS:Ag:Cu* (P-2).

VI

DISCUSSION

As shown in Table I, the luminescent peak energies of all luminophors, except *ZnS:Ag:Cu* and *ZnCdS:Ag*, were the same for both ultra-violet and ion excitation within the experimental limits. For *ZnCdS:Ag*, the ionoluminescent peak energies were about 0.01 - 0.02 eV higher than those of the photoluminescent peak energies. This may or may not be due to the uncertainty in positions of the luminescence peaks for ionoluminescent spectra caused by the dark current of the photomultiplier. However, for *ZnS:Ag:Cu*, especially the P-2 luminophor, the energy shift became as large as $\sim$ 0.03 eV. Unfortunately, some trouble occurred with the paper tape punch of the multi-channel scaler at the time the improved experiments were carried out. It is thus not possible to check these peak energies more accurately and whether the energy shift observed previously was due to the deterioration of the luminophors is not yet certain. If these checks were made and the effect of the ion dosage on the spectra of the other luminophors investigated, a more fruitful result might be obtained.

It is noted from Fig. 9 that the blue peak of *ZnS:Ag:Cu* shows a relatively higher emission intensity for the stimulation light of higher quantum energy. The same phenomenon was observed when the excitation intensity was increased for a particular sample excited by an ultra-violet light of a particular wavelength. However, the arrangement for observing the photoluminescent spectra was not able to cover

more than three orders of magnitude in excitation intensities. Thus it was not possible to carry out more satisfactorily an experiment similar to that done by Shionoya *et al.*[21] to look for the peak energy shift with increasing excitation intensity.

It is apparent from the previous section that the emission spectrum of the doubly activated *ZnS* luminophor depends strongly on such parameters as ion energy, ion mass, ion charge state and ion dosage. In this section, an attempt is made to isolate the effects of the various parameters.

In order to determine the effect of ion energy on the emission spectrum, it is necessary to choose a particular dosage for each specific ion and energy. Since the R *versus* D curves for the ions showed maxima at particular dosages, it was considered that R_{max}, the maximum ratio of the blue to green peaks, would be an indication of the energy dependence. Fig. 20 is a plot of R_{max} *versus* energy, E, for hydrogen, nitrogen, neon and argon. Although there is a considerable uncertainty in the exact shape of the curves obtained due to the uncertainty of the peak positions in Figs. 15, 17-19, it is apparent that R_{max} increases with ion energy and decreases with increasing ion mass. These observations are in qualitative agreement with the results obtained by other workers, i.e.,

> "In general, increasing the excitation density in the phosphor volume penetrated by the excitant decreases the output of the long-wave emission bands relative to that of the short-wave emission bands in complex band emission spectra. This behavior is opposite to the effect of increasing the temperatures of the luminescing phosphors."[31]

If the energy of a particular ion is increased, the excitation should

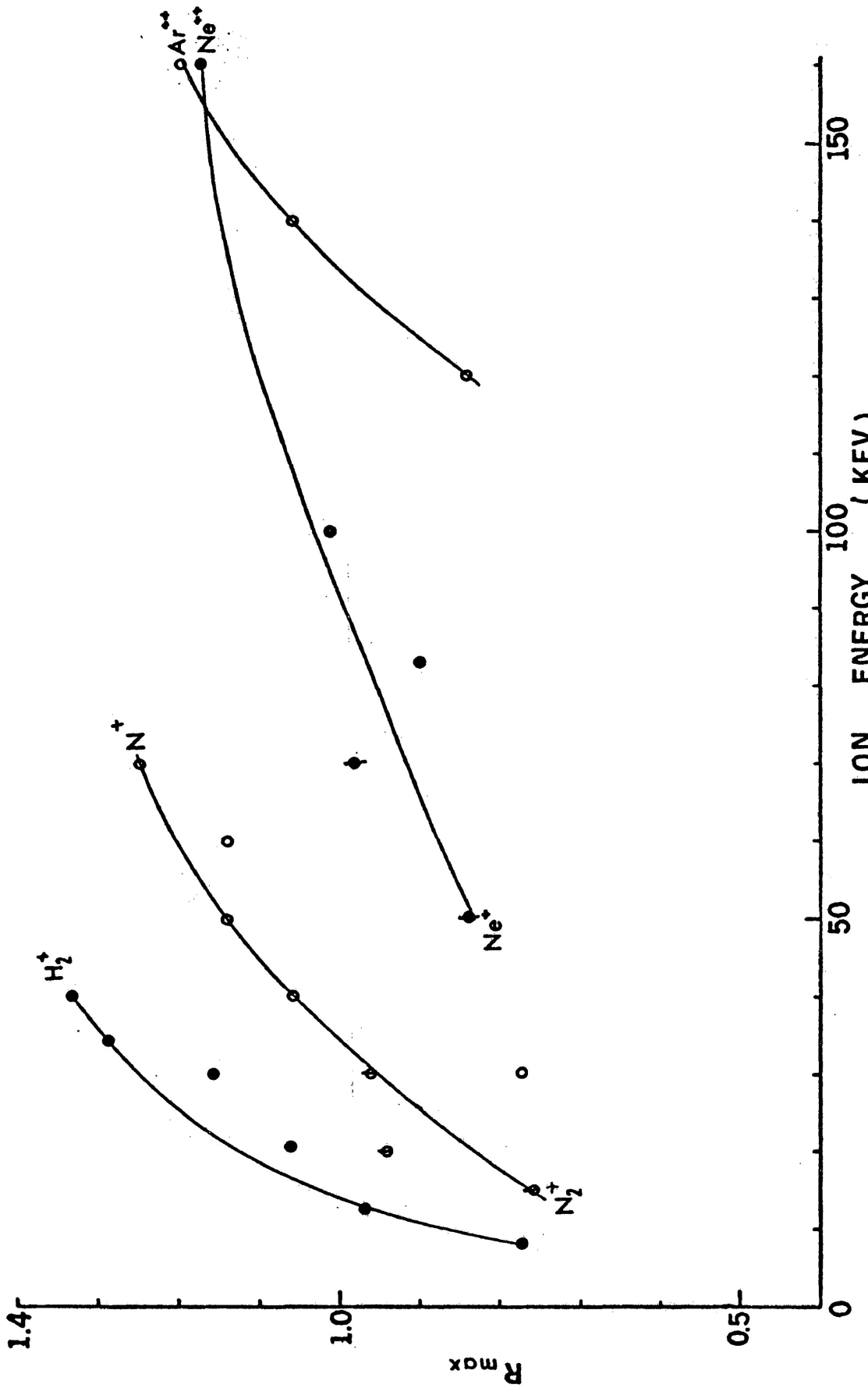

Fig. 20. Maximum ratio of the blue to green peak heights for *ZnS:Ag:Cu* (P-2) under ion excitation.

increase in proportion to the electronic stopping cross section, S_e, or as $E^{\frac{1}{2}}$ (see Eqn. III.8). Thus an increase in ion energy should produce an increase in R_{max}. S_e also increases as the ion mass increases and thus one might expect R_{max} to increase with ion mass at a given energy. This, however, would exclude the effect of the nuclear stopping cross section, S_n, which is a measure of the energy transferred to the crystal lattice. As the projectile mass is increased, S_n increases and thus a fairly intense local heating is expected in the region of the excitation. For the heavier ions, the increase in local temperature could successfully compete with the increased excitation and reduce R_{max}. Table II shows the electronic and nuclear stopping powers, $(dE/dX)_e$ and $(dE/dX)_n$, as well as estimates of the ranges along the path for various projectiles traversing *ZnS* with energy at 50 KeV. It is seen from the table that while the electronic stopping power increases by a factor of about 20 from *H* to *Ar*, the nuclear stopping power increases by more than three orders of magnitude.

The values of the doses for which R_{max} occurs vary strongly from ion to ion and considerably with energy for a particular ion. Since the rate of deterioration also varies considerably for changes in mass and energy, the following comparison was made. Fig. 21 is a plot of L/L_0, a measure of the deterioration, for the dose where R_{max} occurs *versus* energy for various ions. Again since the position of R_{max} is not well defined, there is considerable uncertainty in the points given. There does not seem to be a correlation between the occurrence of the maximum and a given percentage deterioration even for a particular ion. The dependence of R on ion dose is a complicated one. As indicated in

TABLE II

Calculated values of the electronic and the nuclear stopping cross section and the total range in ZnS at 50 KeV

	$(dE/dX)_e$	$(dE/dX)_n$	X
^{1}H	10.1×10^{7} eV / cm	0.475×10^{7} eV / cm	8030 Å
^{4}He	113	5.79	6277
^{14}N	193	121	1781
^{20}Ne	218	251	1142
^{40}Ar	239	773	543

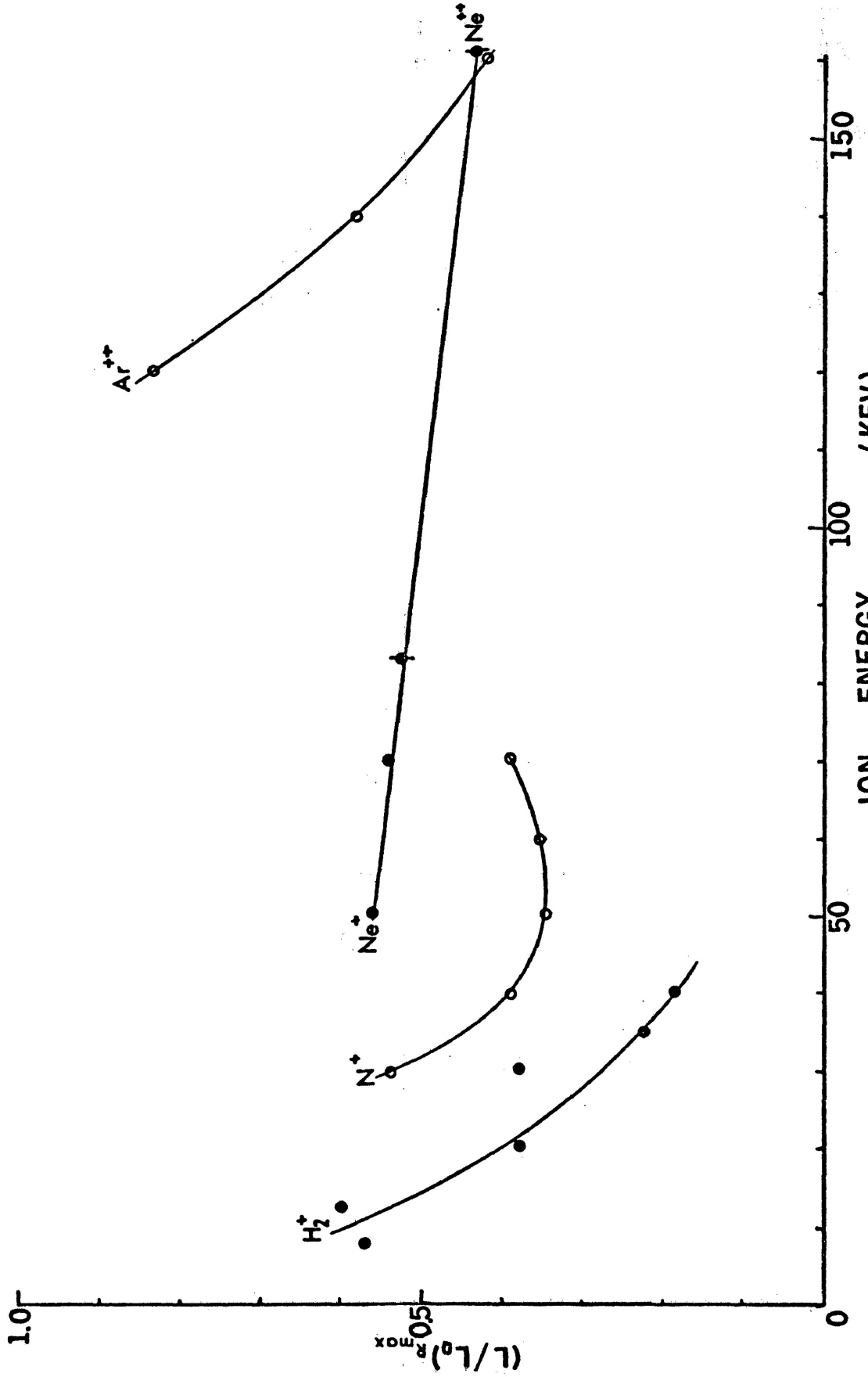

Fig. 21. L/L_0 for the dose where R_{max} occurs *versus* ion energy for *ZnS:Ag:Cu* (P-2) luminophor.

Section III, luminescence of this type is attributed to the recombination of the electron-hole pairs *via* chlorine coactivator levels just below the conduction band and acceptor levels produced either by *Cu* or *Ag* fairly high above the valence band. The deterioration of the luminophor with ion dose is thought[22] to be due to the creation of defects which become the centers for radiationless recombination and thus reduce the efficiency of the luminophor.

As indicated in Fig. 22, the light output increases rather than decreases for low energy heavy ions and for high energy hydrogen ions. This behavior is not simple. A plot of L/L_0 *versus* D first decreases as it normally would and then increases at a similar rate until it reaches what appears to be a maximum. Such behavior was observed for H^+, N_2^+, Ne^+, Ar^+ and Ar^{++} and thus it does not seem to be due to the implanted projectiles acting as activators. The phenomenon was not studied in detail, although it indicated that some rather complicated processes were taking place. It appears that ions not only produce defects which reduce the efficiency of the luminophor, but are also able to enhance the emission spectra. The way in which a particular ion behaves depends strongly on its energy. Perhaps at low energy a heavy incident ion could not transfer enough of its energy to the lattice atoms to produce defects, but expends its energy mainly in heating the lattice and perhaps annealing the defects already present near the surface of the luminophor. The reverse would be true for H^+ since the importance of the nuclear stopping cross section decreases with increasing energy. Another explanation may be made if one considers the effect of traps. The range along the path for

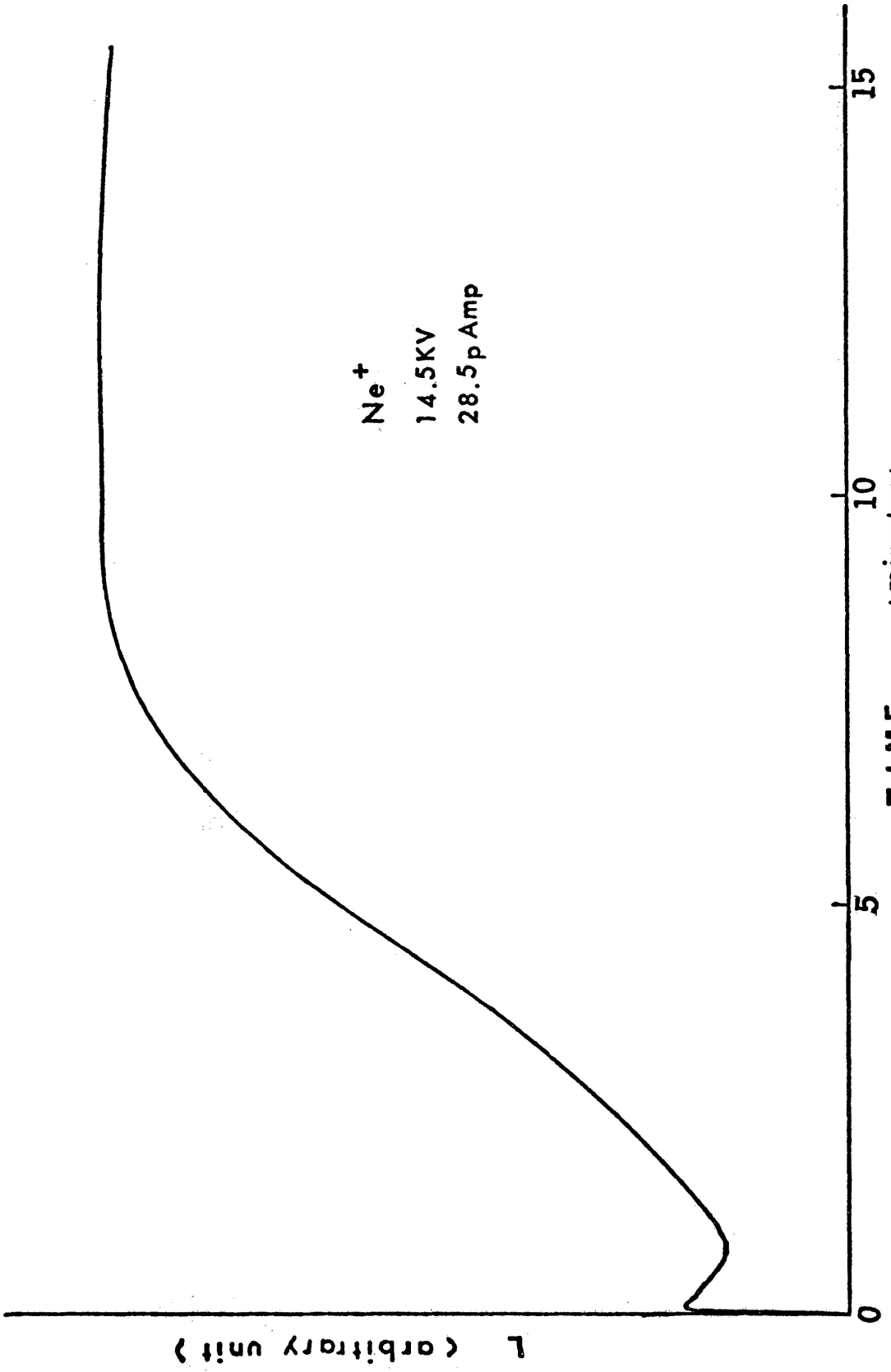

Fig. 22. Light output *versus* time for *ZnS:Ag:Cu* (P-2) excited by 14.5 KV Ne^+ ions.

^{20}Ne at 10 KeV is only about 200 Å, its projected range is much less. This means that the electron-hole pairs created by a low energy ion are formed in a localized region, the dimensions of which are much less than the ambipolar diffusion length ($\sim$ 1000 Å) of the electron-hole pairs. Thus the volume of the luminophor influenced by a particular ion is much larger than the volume swept out by the ion itself. If the former region contains a fair number of long-lived electron traps, then the luminescence can be expected to grow with time until the traps are filled, at which time it will reach an equilibrium. Since the number of electron-hole pairs produced by an ion increases as E increases in the energy range covered, the higher energy ions will fill the traps much more quickly than the lower energy ions and thus the time taken to fill the traps can be reduced to such an extent that the effect is not noticed under the present experimental conditions. This explanation should be valid only for heavy ions and not for the explanation of the growth of luminescence for H^+ at high energy.

VII

CONCLUSIONS

The following conclusions may be drawn from the work done. The energies of the emission peaks of the luminophors studied are not sensitive to the energy or mass of the incident projectile. The energies of the peaks produced by ionoluminescence are the same as those produced by photoluminescence. The ratio of the intensities of the two emission peaks in *ZnS:Ag:Cu* (P-2) depends strongly on the energy, the mass and the dosage of the ion used to excite the emission. The behavior is not understood and would require a deeper knowledge of the defects produced by ion bombardment for its explanation.

APPENDIX I

```
MCS: PROC OPTIONS(MAIN);
DCL A CHAR(80)                ,N(0:1023) BIN FIXED(31,0) INIT((1024)0B),
SE CHAR(5),
DA CHAR(8),
SYSPUNCH FILE SEQUENTIAL OUTPUT,
TAPE FILE SEQUENTIAL INPUT;
ON TRANSMIT(TAPE) ;
ON ENDFILE(SYSIN) STOP;
GET LIST(DW,NG,K);
LS:
GET LIST(DA,SE,KI,KF);
DISPLAY ('*****MOUNT PAPER TAPE '||SE||' ON 007*****');
ON ENDPAGE(SYSPRINT) BEGIN;
IP=IP+1;
PUT PAGE EDIT('*** MULTICHANNEL SCALING ***','TAPE ',SE,
'DATE: ',DA,
'PAGE',IP) (A,X(10),A,A(5),
X(41),2 A,X(10),A,F(3));
PUT SKIP(3);
END;
ON CONV BEGIN;
PUT SKIP(5) EDIT('ERROR IN PAPER TAPE',A,'COUNTS ASSUMED AS:',A)
       (3 (A,SKIP(2)),A(4));
IF II<=KL THEN DO;
PUT EDIT(
(N(II) DO II=KI TO KL))(10 F(7));
GOTO E1;      END;
IF II>KN THEN DO;
PUT EDIT(
(N(II) DO II=KN+1 TO KF))(10 F(7));
GOTO E3;       END;
PUT EDIT(
(N(II) DO II=I TO I+9))(10 F(7));
KM=I+1010B;
GOTO E2;
END;
READ FILE(TAPE) INTO (A);
A='PUNCHED CARDS FOR TAPE '||SE||'                          DATE: '||DA;
WRITE FILE(SYSPUNCH) FROM (A);
KL=KI+1001B-MOD(KI,1010B);
READ FILE(TAPE) INTO (A);
WRITE FILE(SYSPUNCH) FROM (A);
GET STRING(A) EDIT ((N(II) DO II=KI TO KL)) (X(4),10 F(7));
E1:
KN=KF-MOD(KF,1010B)-1B;
KM=KL+1B;
E2:
DO I=KM   TO KN BY 1010B;
READ FILE(TAPE) INTO (A);
WRITE FILE(SYSPUNCH) FROM (A);
GET STRING(A) EDIT ((N(II) DO II=I TO I+9)) (X(4),10 F(7));
END;
READ FILE(TAPE) INTO (A);
WRITE FILE(SYSPUNCH) FROM (A);
GET STRING(A) EDIT ((N(II) DO II=KN+1 TO KF)) (X(4),10 F(7));
E3:
CLOSE FILE(TAPE);
```

APPENDIX I (continued)

```
IP=0B;
SIGNAL ENDPAGE(SYSPRINT);
PUT SKIP EDIT (KI , (N(II) DO II=KI TO KL)) (P'9999',10 F(7));
DO I=KL+1B TO KN BY 10108;
PUT SKIP EDIT (I,   (N(II) DO II=I TO I+9)) (P'9999',10 F(7));
END;
I=KN+1B;
PUT SKIP EDIT (I,   (N(II) DO II=I    TO KF)) (P'9999',10 F(7));
ON CONV BEGIN;
PUT PAGE;
GOTO LS;
END;
EF:
GET LIST(KI,KF,W,C);
SIGNAL ENDPAGE(SYSPRINT);
KM=KF-KI;
A1:BEGIN;
DCL NB(KM) BIN FIXED (31,0) DEF N(KI+1SUB),B(KM);
ON CONV SYSTEM;
ON ENDPAGE(SYSPRINT) ;
B=(NB-NG)/C;
BM=B(1);
DO J=2 TO KM;
IF B(J)>BM THEN BM=B(J);
END;
PUT      EDIT('0        1|0       2|0       3|0       4|0       5|0
   6|0       7|0       8|0       9|0       100') (X(17),A);
IF DW>0 THEN DO;
KI=1B;  KF=KM;    KL=1B;    END;
ELSE DO;
KI=KM;  KF=1B;    KL=-1B;   END;
NB=B/BM*100;
DO J=KI TO KF BY KL;
PUT SKIP EDIT (W+DW*(J-1),B(J),' +',NB(J))
(F(5),E(11,3),X(NB(J)),A,COL(119));
END;
PUT SKIP EDIT('0        1|0       2|0       3|0       4|0       5|0
   6|0       7|0       8|0       9|0       100') (X(17),A);

PUT PAGE;
KN=KM-MOD(KM,K);
DO I=0B TO KN-10B BY K;
PUT SKIP(3) EDIT((W+DW*J DO J=I TO I+K-1B ),(B(J) DO J=I+1B TO I+K))
((K) F(10),SKIP,(K) E(10,2));
END;
IF KM>KN THEN
PUT SKIP(3) EDIT((W+DW*J DO J=KN    TO KM-1B),(B(J) DO J=KN+1B TO KM))
((KM-KN) F(10),SKIP,(KM-KN) E(10,2));
          END A1;
GOTO EF;
END;
```

APPENDIX II

ADAPTED FROM FUNCTION DSTAT IN STP1
E. ARMITAGE; COMPUTING CENTER; U. OF ALBERTA

```
    ∇ DSTAT X;R;MAX;MIN;N;MEAN;VAR;SD;MD;MED;MODE;V;M
[1]   R←(MAX←X[⍴X])-MIN←(X←X[⍋X])[1]
[2]   SD←(VAR←(+/(X-MEAN←(+/X)÷N)*2)÷(N←⍴X)-1)*0.5
[3]   MD←(+/|X-MEAN)÷N
[4]   MED←0.5×+/X[(⌈N÷2),1+⌊N÷2]
[5]   →(N>⍴MODE←((⍴V)⍴(⍳M)≤1)/V←X[(V=M←⌈/V←+/X∘.=X)/⍳⍴X])/7
[6]   MODE←⍳0
[7]   ('SAMPLE SIZE          ';N)
[8]   ('MAXIMUM              ';MAX)
[9]   ('MINIMUM              ';MIN)
[10]  ('RANGE                ';R)
[11]  ('MEAN                 ';MEAN)
[12]  ('VARIANCE             ';VAR)
[13]  ('STANDARD DEVIATION   ';SD)
[14]  'STANDARD ERROR        ';SD÷N*0.5
[15]  ('MEAN DEVIATION       ';MD)
[16]  ('MEDIAN               ';MED)
[17]  ('MODE                 ';MODE)
[18]  ('PEARSONIAN SKEW      ';((+/(X-MEAN)*3)÷N-1)÷SD*3)
[19]  ('KURTOSIS             ';((+/(X-MEAN)*4)÷N-1)÷SD*4)
    ∇
```

REFERENCES

[1]H. W. Leverenz, *An Introduction to Luminescence of Solids* (Dover: New York, 1968).

[2]W. Hanle and K. H. Rau, Z. Physik, 133, 297 (1952).

[3]P. I. Richards and E. E. Hays, Rev. Sci. Instr., 21, 99 (1950).

[4]C. F. Eve and H. E. Duckworth, Can. J. Phys., 36, 104 (1958).

[5]A. van Wijngaarden, D. J. Bradley and N. M. A. Finney, Can. J. Phys., 43, 2180 (1965).

[6]L. Hastings, P. R. Ryall and A. van Wijngaarden, Can. J. Phys., 45, 2333 (1967).

[7]V. V. Makarov and N. N. Petrov, Soviet Physics - Solid State, 10, 154 (1968).

[8]A. von Hippel, Z. Physik, 101, 680 (1936).

[9]J. L. Birman, Phys. Rev., 109, 810 (1958).

[10]S. Shionoya, T. Koda, K. Era and H. Fujiwara, J. Phys. Soc. Japan, 19, 1157 (1964).

[11]M. Schön, Z. Physik, 119, 463 (1942).

[12]H. A. Klasens, Nature, 158, 306 (1946).

[13]J. Lambe and C. C. Klick, Phys. Rev., 98, 909 (1955).

[14]J. Lambe, Phys. Rev., 100, 1586 (1955).

[15]J. S. Prener and F. E. Williams, J. Electrochem. Soc., 103, 342 (1956).

[16]F. E. Williams, J. Opt. Soc., 47, 869 (1957).

[17]J. J. Hopfield, D. G. Thomas and M. Gershenzon, Phys. Rev. Letters, 10, 162 (1963).

[18]D. G. Thomas, M. Gershenzon and A. Trumboref, Phys. Rev., 133, A269 (1964).

[19]D. G. Thomas, J. J. Hopfield and W. M. Augustyniak, Phys. Rev., 140, A202 (1965).

[20]F. M. Ryan and R. C. Miller, Phys. Rev., 148, 858 (1966).

[21]K. Era, S. Shionoya and Y. Washizawa, J. Phys. Chem. Sol., 29, 1827-1843 (1968).

[22]A. van Wijngaarden and L. Hastings, Can. J. Phys., 45, 3803 (1967).

[23]J. Lindhard and M. Scharff, Phys. Rev., 124, 128 (1961).

[24]J. Lindhard, V. Nielsen, M. Scharff and P. V. Thomas, Kgl. Danske Videnskab. Selskab Mat. Fys. Medd., 33, 10 (1963).

[25]J. Lindhard, M. Scharff and H. E. Schiøtt, Kgl. Danske Videnskab. Selskab Mat. Fys. Medd., 33, 14 (1963.

[26]J. Lindhard, V. Nielsen and M. Scharff, Kgl. Danske Videnskab. Selskab Mat. Fys. Medd., 36, 10 (1968).

[27]L. Hastings, Department of Physics, Lakehead University, Thunder Bay, Ontario. Private communication.

[28]H. W. Leverenz, RCA Review, 7, 199 (1946).

[29]M. J. Brines, Electronic Phosphor Engineering, General Electric Co., U.S.A. Private communication.

[30]H. W. Leverenz, *An Introduction to Luminescence of Solids* (Dover: New York, 1968).